

1 Impacts of soil management and climate on saturated
2 and near-saturated hydraulic conductivity: analyses of
3 the Open Tension-disk Infiltrometer Meta-database
4 (OTIM)

5 **Authors**

6 Guillaume Blanchy¹, Lukas Albrecht², Gilberto Bragato³, Sarah Garré¹, Nicholas Jarvis⁴, John Koestel^{2,4}

7
8 ¹*Flanders Research Institute for Agriculture, Fisheries and Food (ILVO), Melle, Belgium*

9 ²*Agroscope, Reckenholzstrasse 191, 8046 Zürich, Switzerland*

10 ³*Council for Agricultural Research and Economics (CREA), Via Po, 14, 00198 Roma, Italy*

11 ⁴*Department of Soil and Environment, Swedish University of Agricultural Sciences (SLU), P.O. Box 7014, 750 07*
12 *Uppsala, Sweden*

13

14 **Corresponding author**

15 John Koestel (johannes.koestel@agroscope.admin.ch)

16

17 **Keywords**

18 hydraulic conductivity, saturated hydraulic conductivity K_s , near-saturated hydraulic conductivity,
19 Kunsat, Knearsat, soil hydraulic properties, infiltration, tension-disk infiltrometer, soil properties, climate,
20 soil, agricultural management practice, pedo-climatic factors, meta-analysis

21 **Abstract**

22 Saturated and near-saturated soil hydraulic conductivities K_h (mm h^{-1}) determine the partitioning of
23 precipitation into surface runoff and infiltration and are fundamental to soils' susceptibility to preferential
24 flow. Recent studies have found indications that climate factors influence K_h , which is highly relevant in
25 the face of climate change. In this study, we investigated relationships between pedo-climatic factors

26 and K_h , and also evaluated effects of land use and soil management. To this end, we collated the Open
27 Tension-disk Infiltrometer Meta-database (OTIM), which contains 1297 individual data entries from 172
28 different publication sources. We analysed a spectrum of saturated and near-saturated hydraulic
29 conductivities at matric potentials between 0 to 100 mm. We found that methodological details like the
30 direction of the wetting sequence or the choice of method for calculating infiltration rates to hydraulic
31 conductivities had a large impact on the results. We therefore restricted ourselves to a subset of 466 of
32 the 1297 data entries with similar methodological approaches. Correlations between K_s and K_h at higher
33 supply tensions decreased especially close to saturation, indicating a different flow mechanism at and
34 very close to saturation as towards the dry end of the investigated tension range. Climate factors were
35 better correlated to topsoil near-saturated hydraulic conductivities at supply tensions ≥ 30 mm than soil
36 texture, bulk density and organic carbon content. We find it most likely that the climate variables are
37 proxies for soil macropore networks created by respective biological activity, pedogenesis and climate
38 specific land use and management choices. Due to incomplete documentation in the source
39 publications of OTIM, we could investigate only a few land use types and agricultural management
40 practices. Land use, tillage system and soil compaction significantly influenced K_h , with effect sizes
41 appearing comparable to the ones of soil texture and soil organic carbon. The data in OTIM show
42 experimental bias is present, introduced by the choice of measurement time relative to soil tillage,
43 experimental design or data evaluation procedures. The establishment of best-practice rules for
44 tension-disk infiltrometer measurements would therefore be helpful. Future studies are needed to
45 investigate how climate shapes soil macropore networks and how land use and management can be
46 adapted to improve soil hydraulic properties. Both tasks require large amounts of new measurement
47 data with improved documentation on soil biology and land use and management history.

48 1. Introduction

49 Climate models predict more frequent extreme weather events such as high intensity rainfall with the
50 onset of global warming. To prevent water runoff and erosion, soils need to be able to conduct
51 sometimes large amounts of water in a short time. It is generally accepted that one key soil property is
52 the saturated hydraulic conductivity K_s (mm h^{-1}), as it determines the partitioning of precipitation into

53 surface runoff and infiltration. A large K_s reduces erosion risks and allows water to infiltrate into deeper
54 soil layers, where it may replenish an important reservoir of plant available water or contribute to
55 groundwater recharge. The hydraulic conductivity of a soil decreases with decreasing water content,
56 i.e. with decreasing water saturation. The hydraulic conductivity in the so-called near-saturated range
57 (between 0 and 100 mm matric tensions) is likewise important. For rainfall intensities smaller than but
58 close to K_s , soils with larger near-saturated hydraulic conductivity K_h (mm h^{-1}) will remain less water-
59 saturated because they are able to conduct the precipitation water in smaller macropores. Therefore,
60 they are less susceptible to preferential flow (Larsbo et al., 2014) by which agrochemicals and other
61 solutes quickly leach towards the groundwater. Moreover, a large K_h also indicates a well-aerated soil,
62 which drains faster and helps air to escape the soil in case of heavy rainfall. This further reduces the
63 risk of surface runoff and erosion as entrapped air strongly decreases soil hydraulic conductivity.

64 Saturated hydraulic conductivity is measured either in the laboratory on small cylinders, usually with
65 diameters < 7 cm (Klute and Dirksen, 1985) or it is acquired from field measurements, either using
66 single or double ring infiltrometer methods (Angulo-Jaramillo et al., 2000). In addition, near-saturated
67 hydraulic conductivities can be measured using a tension disk infiltrometer. The method is designed as
68 a field method, but has been occasionally applied in the laboratory. Using a tension disk infiltrometer,
69 hydraulic conductivities at supply tensions between ca. 0.5 and ca. 60 to 150 mm can be obtained,
70 depending on the specifications of the infiltrometer. All measurement techniques for saturated and near-
71 saturated hydraulic conductivity are laborious, time-consuming and constrained to a relatively small soil
72 volume.

73 It is necessary to develop pedotransfer functions to estimate soil hydraulic conductivities for large-scale
74 modelling applications, as we cannot measure everywhere (Bouma, 1988; Van Looy et al., 2017;
75 Wösten et al., 2001). The development of a pedotransfer function requires a database from which it can
76 be derived. For example, the well-known pedotransfer function ROSETTA (Schaap et al., 2000) is
77 based on the open UNSODA database (Nemes et al., 2001). The equations published in Tóth et al.,
78 2015 are derived from the proprietary EU-HYDI database (Weynants et al., 2013). The pedotransfer
79 functions of Jarvis et al. (2013) are based on an unpublished meta-database containing tension-disk

80 infiltrometer data. Collecting published measurements of saturated and near-saturated hydraulic
81 conductivity measurements into meta-databases and pairing them with other existing databases is
82 essential to develop pedotransfer functions. A notable example is the SWIG database (Rahmati et al.,
83 2018) that collates more than 5000 datasets from soil infiltration measurements, covering the entire
84 globe. Another big effort in collecting information on saturated hydraulic conductivity is the newly
85 published SoilKsatDB (Gupta et al., 2021a), which combines saturated hydraulic conductivity data from
86 several large databases, amongst others UNSODA and SWIG, together with additional measurements
87 published in independent scientific studies. However, none of the databases cited above provide open-
88 access infiltration measurements at tensions near-saturation ($h > 0$ mm), which limits their use to the
89 estimation of saturated hydraulic conductivity.

90 While reasonably good estimations of K_s from easy-to-measure or readily available site properties
91 appear to be possible for peat soils (Morris et al., 2022), pedotransfer functions for K_s of mineral soils
92 exhibit poor predictive performance with coefficients of determination R^2 not exceeding 0.25. (Weynants
93 et al., 2009; Jorda et al., 2015). Early approaches, like HYPRES (Wösten et al., 1999) and ROSETTA,
94 focused solely on soil properties like texture, bulk density and organic carbon content as predictors for
95 K_s . At the time, it was not sufficiently recognized that soil K_s is mostly determined by the morphology of
96 macropore networks, especially in finer-textured soils (Vereecken et al., 2010; Koestel et al., 2018;
97 Schlüter et al., 2020). A pedotransfer function for K_s requires therefore ideally a database that contains
98 direct information on the macropore network itself. But since such measures are even more
99 cumbersome and time-consuming to obtain (e.g. by X-ray tomography) than measuring hydraulic
100 conductivity itself, it is more reasonable and makes more sense to use proxies from which the
101 macrostructure in a soil can be inferred. Ideal candidates would be root growth and the activity of soil
102 macrofauna, which both strongly determine the development of macropore networks in soil (Meurer et
103 al., 2020). However, they are difficult to measure. Proxies that are more promising are land use and
104 farming practises, such as tillage or soil compaction due to trafficking. Plant growth and soil macrofauna
105 in turn are influenced by the local climate. The climate also sets boundaries for the land use and the
106 associated soil management practices, and thus provides feedback to root growth and macro-faunal
107 activity. Wetting and drying cycles and thus the formation and closure of cracks also are regulated by

108 the climate as is splash erosion and soil crusting. It is therefore not surprising that climate variables
109 typically are correlated with saturated and near-saturated hydraulic conductivities (Jarvis et al., 2013;
110 Jorda et al., 2015; Hirmas et al., 2018; Gupta et al., 2021b). Jorda et al., 2015 found that land use itself
111 was the most important predictor for saturated hydraulic conductivity.

112 The time of measurement of the hydraulic conductivity (or soil sampling) also has a crucial impact. In
113 an agricultural soil, the hydraulic properties of a freshly prepared seedbed differ from those measured
114 later at harvest. Several studies have demonstrated the evolution of hydraulic conductivity with time
115 (Messing and Jarvis, 1990; Messing and Jarvis, 1993; Bodner et al., 2013; Sandin et al., 2017). Soil
116 management options (such as tillage or the use of cover crops) actively influence the soil saturated and
117 near-saturated hydraulic conductivity. Information on their impact is therefore especially important, but
118 so far has hardly been investigated in meta-studies.

119 In this study, we focused on quantifying the effect of soil management practices on soil saturated and
120 near-saturated hydraulic conductivity, K_h . We also investigated relationships between K_h and other
121 potentially important influencing factors like soil properties, local climate and details of the measurement
122 methods. In this process, we expanded and published the previously unpublished meta-database on
123 tension-disk infiltration measurements that was first reported by Jarvis et al. (2013). We referred to this
124 database as OTIM in the following (Open Tension-disk Infiltrometer Meta-Database). It complements
125 the currently available public databases on hydraulic conductivities, which are strongly based on
126 laboratory measurements or ring infiltrometer methods.

127 2 Material and Methods

128 2.1 Meta-Database, OTIM

129 2.1.1 Data collection

130 The first version of OTIM was compiled for the study by Jarvis et al., 2013. The original database
131 contained 753 tension-disk infiltrometer data entries collated from 124 source publications, covering
132 144 different locations around the globe. We have extended this database by 544 new tension-disk
133 infiltrometer data entries from 48 additional studies that had been published after 2012. The search for

134 publications was carried out between 2021-05-31 and 2021-06-23 using the queries and search engines
 135 detailed in Table A1.

136 We found 115 publications containing tension-disk infiltrometer measurements published in 2013 or
 137 later. We retained the data for further analysis when (i) K_h or the infiltration rate was measured at more
 138 than two tensions larger or equal to 5 mm and (ii) sufficient meta-data on soil and site properties (at
 139 least soil texture) as well as soil management practices (at least land use and tillage) were available. If
 140 a publication only reported infiltration rates, we calculated hydraulic conductivity using the method of
 141 Ankeny et al. (1991). Only 45 of the 115 publications fulfilled the above-mentioned criteria. Table A2
 142 summarises how many papers were rejected and for which reasons. For 27 of the 45 retained studies,
 143 we digitised the published K_h values from figures using WebPlotDigitizer (open-source web-based
 144 software created by Ankit Rohatgi, <https://automeris.io/WebPlotDigitizer/>). For cases in which K_h
 145 measurements were mentioned in a publication, but the results were not reported, we contacted the
 146 corresponding authors. We received the data in this fashion for three of these publications (Alletto et
 147 al., 2015; Larsbo et al., 2016a; Meshgi and Chui, 2013). The new studies containing data were added
 148 to the OTIM database are summarised in Table 1.

149 **Table 1: List of new entries added to the Jarvis et al., 2013 database.**

Reference	Land use	Tillage	Compaction	Sampling time	Data entries
Alagna et al., 2015	grassland	no tillage	not compacted	consolidated soil	1
Alletto et al., 2015	arable	conventional tillage	unknown	consolidated soil	60
Bagarello et al., 2014	arable	no tillage conventional tillage	unknown	unknown	10

Baranian Kabir et al., 2020	grassland arable	no tillage	not compacted compacted	unknown consolidated soil	4
Bátková et al., 2020	arable	reduced tillage no tillage conventional tillage	unknown	consolidated soil soon after tillage	12
Bodner et al., 2013	arable	no tillage	unknown	soon after tillage consolidated soil	12
Bottinelli et al., 2013	arable	unknown conventional tillage reduced tillage no tillage	unknown	consolidated soil	10
Costa et al., 2015	arable	conventional tillage reduced tillage no tillage	not compacted	consolidated soil	3
De Boever et al., 2016	grassland	no tillage	not compacted	unknown	6
Tóth et al., 2014	arable	conventional tillage	not compacted compacted	consolidated soil	2
Etana et al., 2013	arable	conventional tillage	not compacted compacted	unknown	2
Fashi et al., 2018	arable	no tillage	compacted not	unknown	8

		reduced tillage conventional tillage	compacted		
Fasinmirin et al., 2018	arable woodland/plantation grassland	conventional tillage no tillage	not compacted compacted	unknown	3
Greenwood, 2016	arable grassland	conventional tillage no tillage	unknown	consolidated soil	4
Hallam et al., 2020	arable	conventional tillage	not compacted	unknown	60
Hardie et al., 2012	arable	no tillage	not compacted	consolidated soil	2
Holden et al., 2014	grassland	no tillage	not compacted	consolidated soil	5
Hyväluoma et al., 2019	arable	conventional tillage	unknown	consolidated soil	4
Iovino et al., 2016	arable grassland woodland/orchard	reduced tillage no tillage	unknown	consolidated soil	3
Kelishadi et al., 2013	arable grassland	reduced tillage no tillage conventional tillage	not compacted	consolidated soil	4
Keskinen et al., 2019	arable	no tillage	unknown	consolidated soil	15

		conventional tillage			
Khetdan et al., 2017	arable	no tillage	unknown	unknown	4
Larsbo et al., 2016a	arable	conventional tillage	not compacted compacted	consolidated soil unknown	5
Lopes et al., 2020	woodland/orchard grassland	no tillage	not compacted	consolidated soil	4
Lozano et al., 2014	arable	no tillage	not compacted	consolidated soil	2
Lozano-Baez et al., 2020	grassland woodland/orchard	no tillage	not compacted	unknown	18
Matula et al., 2014	grassland	no tillage	unknown	unknown	3
Miller et al., 2018	arable	conventional tillage	unknown	consolidated soil	10
Mirzavand, 2016	arable	conventional tillage reduced tillage no tillage	unknown	consolidated soil	12
Pulido Moncada et al., 2014	arable grassland	conventional tillage no tillage	unknown	unknown	4
Rahbeh, 2019	arable	conventional	unknown	consolidated	69

		tillage		soil	
Rienzner and Gandolfi, 2013	arable	conventional tillage	not compacted	unknown consolidated soil	18
Sandin et al., 2017	arable	conventional tillage	not compacted compacted	consolidated soil unknown	7
Soracco et al., 2015	grassland	conventional tillage	not compacted compacted	unknown	3
Soracco et al., 2019	arable	conventional tillage no tillage	unknown	consolidated soil	6
Wang, 2021	arable	conventional tillage	unknown	soon after tillage consolidated soil	25
Wanniarachchi et al., 2019	arable	conventional tillage	unknown	consolidated soil	6
Yu et al., 2013	grassland	no tillage	unknown	unknown	11
Yusuf et al., 2017	arable	no tillage	not compacted	consolidated soil	1
Yusuf et al., 2020	arable	no tillage	not compacted	consolidated soil	5

Zeng et al., 2013	woodland/orchard	conventional tillage	unknown	consolidated soil	20
Zeng et al., 2012	grassland	no tillage	unknown	consolidated soil	6
Zhang et al., 2013	grassland arable	no tillage unknown	unknown	consolidated soil	6
Zhang et al., 2014	arable	conventional tillage	unknown	consolidated soil	4
Zhang et al., 2016	woodland/orchard arable	no tillage conventional tillage	unknown not compacted	consolidated soil soon after tillage	24
Zhang et al., 2021	grassland woodland/orchard arable	no tillage conventional tillage	unknown	consolidated soil	4
Zhao et al., 2014	arable grassland	conventional tillage no tillage	not compacted	unknown	12
Zhou et al., 2015	arable grassland woodland/orchard	conventional tillage no tillage	not compacted	soon after tillage	3

150

151 In addition to adding data from new publications to OTIM, we also revisited the studies contained in the
152 original version of the database and collected additional information on soil management practices
153 associated with the measured data. For each soil management option, OTIM contains two columns. In
154 the first column, the information as given in the source publication is stored. The second column

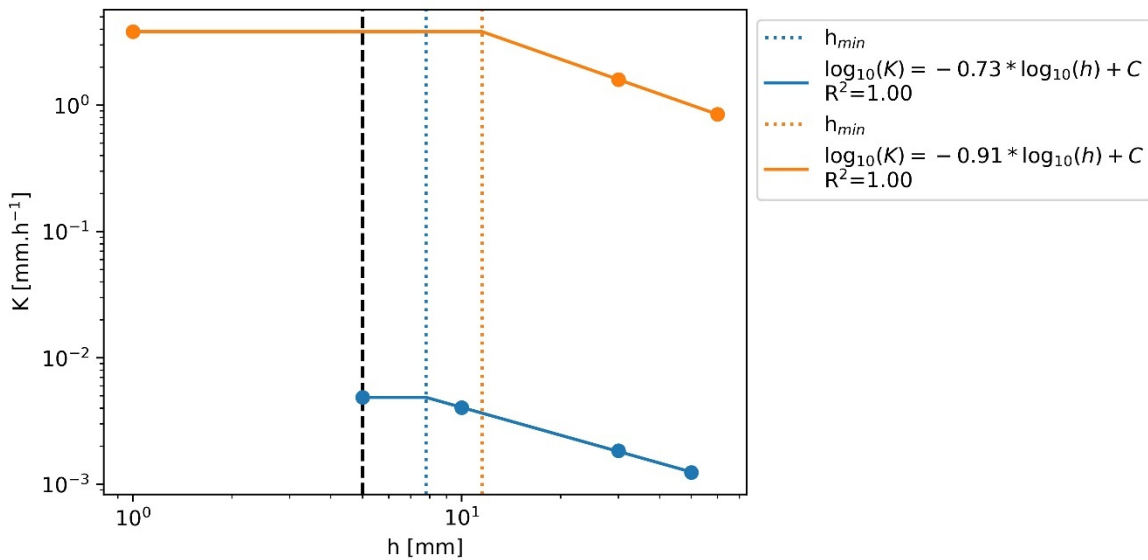
155 summarises this information into a few classes, which were subsequently used in the meta-analysis. In
156 this study, we investigated effects of land use, tillage system, soil compaction and day of measurement
157 relative to the latest tillage operation on the field. A compaction class was assigned to a data entry only
158 if the plot had been described as 'compacted' or 'not compacted' in the source publication. 'Compacted'
159 data entries corresponded, for example, to infiltration measurements in wheel tracks or on plots of a
160 compaction experiment. The day of measurement relative to tillage was also included, with the data
161 labelled 'freshly tilled' when the authors in the source publication stated that the measurements had
162 taken place soon after tillage. Otherwise, it was assumed that the soil already had time to consolidate
163 before the infiltration measurements were carried out. All soil texture data were mapped onto the USDA
164 classification system using the method proposed in Nemes et al. (2000).

165 2.1.2. Climate data and soil classification

166 The climatic data entries provided in the database were created using the bioclimatic raster data
167 (BioClim) provided by WorldClim (worldclim.org). The data was averaged across the years 1970 to
168 2000 and had a 30 arc second resolution (~1 km²; Fick and Hijmans, 2017). The available climate
169 variables were mean annual temperature and precipitation, the mean temperature as well as mean
170 precipitation of the warmest, coldest, wettest and driest quarter and month, respectively, the
171 isothermality, the mean diurnal and annual temperature range, the seasonality for temperature and
172 precipitation. Besides the bio-climatic data in WorldClim we included the aridity index (here defined as
173 the annual precipitation divided by the potential evapotranspiration) as well as the average annual
174 potential evapotranspiration (ET₀). Both were inferred from the "Global Aridity Index and Potential
175 Evapotranspiration Climate Database v2" that is based on the WorldClim database (Trabucco and
176 Zomer, 2019). The World Reference Base (WRB) soil type was also extracted from the source
177 publications. When it was not reported, the SoilGrids database by ISRIC (Poggio et al., 2021) was used
178 to infer it. The map contained information about the main soil type regarding the WRB classes (IUSS
179 Working Group WRB, 2015). The most probable soil type was chosen for each location. For all
180 discussed climate and soil maps, the python package "rasterio" (v1.2.10) was used to collect the
181 variables from the corresponding raster cell at the location coordinates given in the source publications.

182 2.1.3 Model fit to infer K_h at near-saturated tensions not measured

183 Tension-disk infiltrometers measure infiltration rates at a specific supply tension (Angulo-Jaramillo et
 184 al., 2000). They consist of a ceramic disk to which a water reservoir and a bubbling tower is attached.
 185 The ceramic disk is saturated and hydraulically connected to the soil by inserting a layer of fine sand
 186 between the disk and the soil surface. The supply tension at the bottom of the ceramic disk is adjusted
 187 by the bubbling tower. The measured unconfined (i.e. three-dimensional) infiltration rates are then
 188 commonly converted to hydraulic conductivities with the aid of the Wooding equation (Wooding, 1968).
 189 Note that unconfined tension-disk infiltrometers cannot provide measurements at a tension of zero, i.e.
 190 K_s . Even if many publications report K_s values obtained from tension-disk infiltrometers, these
 191 measurements must have been conducted at tensions slightly larger than zero, as water would
 192 otherwise have freely leaked out of the tension disk. For this reason, we set the tensions for K_s
 193 measurements to 1 mm, but still referred to these data as saturated hydraulic conductivity. Note that
 194 we discuss matrix potentials in terms of tensions (negative pressures) throughout this manuscript. For
 195 convenience, we denote K_h at a specific tension by replacing the subscript h by the tension value in
 196 mm. For example, K_{100} denotes K_h at a supply tension of 100 mm.



197

198 **Figure 1: Two examples for the linear fit in log-log space. The colors denote two different**
 199 **measured tension series. The filled circles correspond to measured K_h , while the lines**
 200 **indicate the interpolation carried out by the model. The bold black dashed line marks a**
 201 **supply tension of 5 mm. K_h at tensions between 0 and 5 mm were assumed to be identical**

202 **to K_s . Reported K_s values were assigned a tension of 1 mm for illustration purposes. The**
203 **equations for the linear part of the fit are shown in the legend. C represents the intercept**
204 **with the y-axis of the linear fit in log-space, h_{min} corresponds to the supply tension at which**
205 **the largest pores in the soil are water-filled.**

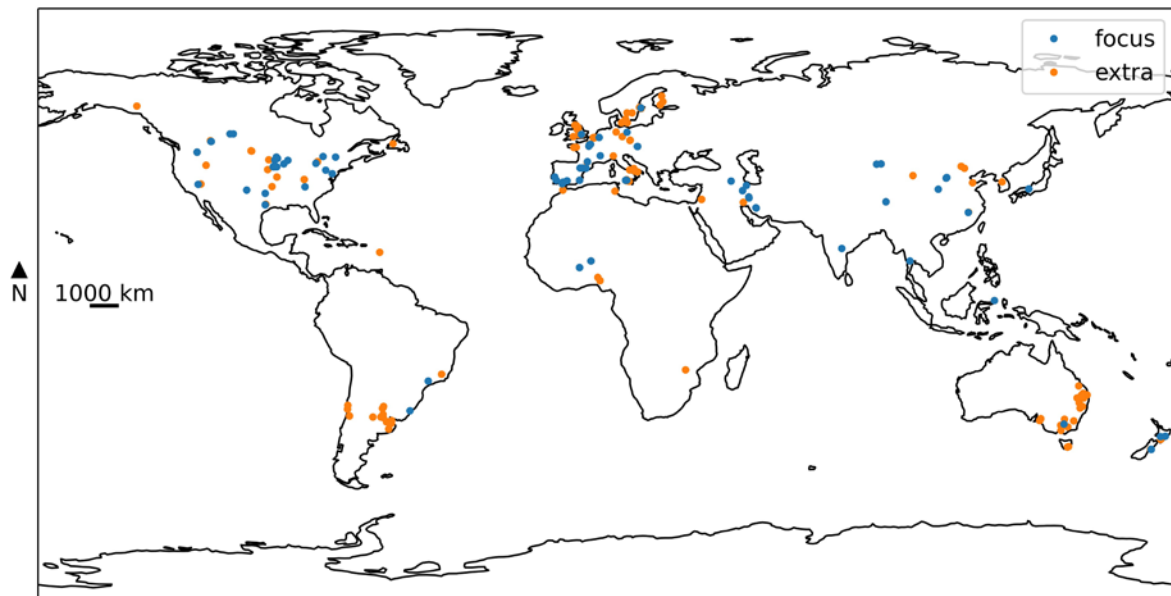
206 Following Jarvis et al., 2013, we interpolated K_h for tensions in-between the ones measured in the
207 source publications. We achieved this by fitting a log-log linear model with a kink at a tension h_{min} , which
208 denotes the tension at which the largest effective pores in the soil are water-filled (see Figure 1).
209 Therefore, $K_h \equiv K_s$ for all tensions $h \leq h_{min}$. If K_s was not measured but instead a K_h value at $h \leq 5$ mm
210 was available, K_s was set to the available K_h value (Figure 1 orange line). In cases where more than
211 one K_h value was measured at a tension smaller or equal to 5 mm (including $h = 0$ mm, i.e. K_s), we
212 averaged them and fixed K_s and K_h for $h \leq h_{min}$ to the average (Figure 1 green line). K_h values at $h > 5$
213 mm were used to fit the log-log linear relationship. The tension at which the fitted log-log slope
214 intersected with K_s defined h_{min} . We used the fitted model to estimate all K_h values for tensions for $10 \leq$
215 $h \leq 100$ mm at 10 mm intervals. The K_h values were only interpolated between the tensions that were
216 measured in the source publication. The only exceptions from this rule were made in the case where a
217 K_h value for a tension of 80 or 90 mm was provided together with at least one other K_h value measured
218 at a smaller tension. Then, the missing K_h values were extrapolated up to a tension of 100 mm. Figure
219 1 shows examples of model fits. Only entries with an R^2 greater or equal to 0.9 were retained in the
220 analysis.

221 2.2 Data availability and spatial coverage

222 Although 92% of the OTIM data are from topsoils, OTIM also contains some data points measured at
223 greater soil depths. In the following meta-analysis, only measurements from the topsoil were included
224 to prevent bias and all datasets measured at soil depths below 200 mm were removed. Last but not
225 least, we found that the relationship between supply tension and K_h was distorted if data entries were
226 included that did not cover the complete tension range from $h = 0$ to 100 mm. Possible reasons for the
227 difficulties to match K_h data from tension series with different lengths are discussed at the beginning of
228 the results and discussion section. Otherwise, we focused on data entries that included K_h values for
229 the complete tension range in the exploratory data analysis and the meta-analyses. The available

230 datasets after these filtering steps correspond to the ones indicated in blue (and termed 'focus') in
231 following figures.

232 Most tension-disk infiltrometer studies were conducted in Europe, North America and Southeast
233 Australia (Figure 2). Clearly, fewer studies have been carried out in Asia, South America and Africa.
234 The lack of datasets from Russia, Mesoamerica, the arctic regions and the tropics is remarkable. This
235 geographical bias is aggravated if only measurements on the topsoil are considered that allow
236 inferences about K_h for the complete range of tensions ($0 \leq h \leq 100$ mm) with a sufficiently good
237 coefficient of determination. Then, all the data entries collected in southern South America and south-
238 eastern Australia were omitted, as well. Overall, the data in OTIM mostly stem from temperate climate
239 regions.



240
241 **Figure 2: Map of the study locations collected in the OTIM. The values are shown for the**
242 **filtered entries ('focus') and in parenthesis for all the entries available in the database**
243 **('focus' and 'extra').**

244 Figure 3 depicts the number of K_h values available for $0 \leq h \leq 100$ mm. These figures represent the
245 hydraulic conductivities derived from the log-log linear model presented above, not the raw data

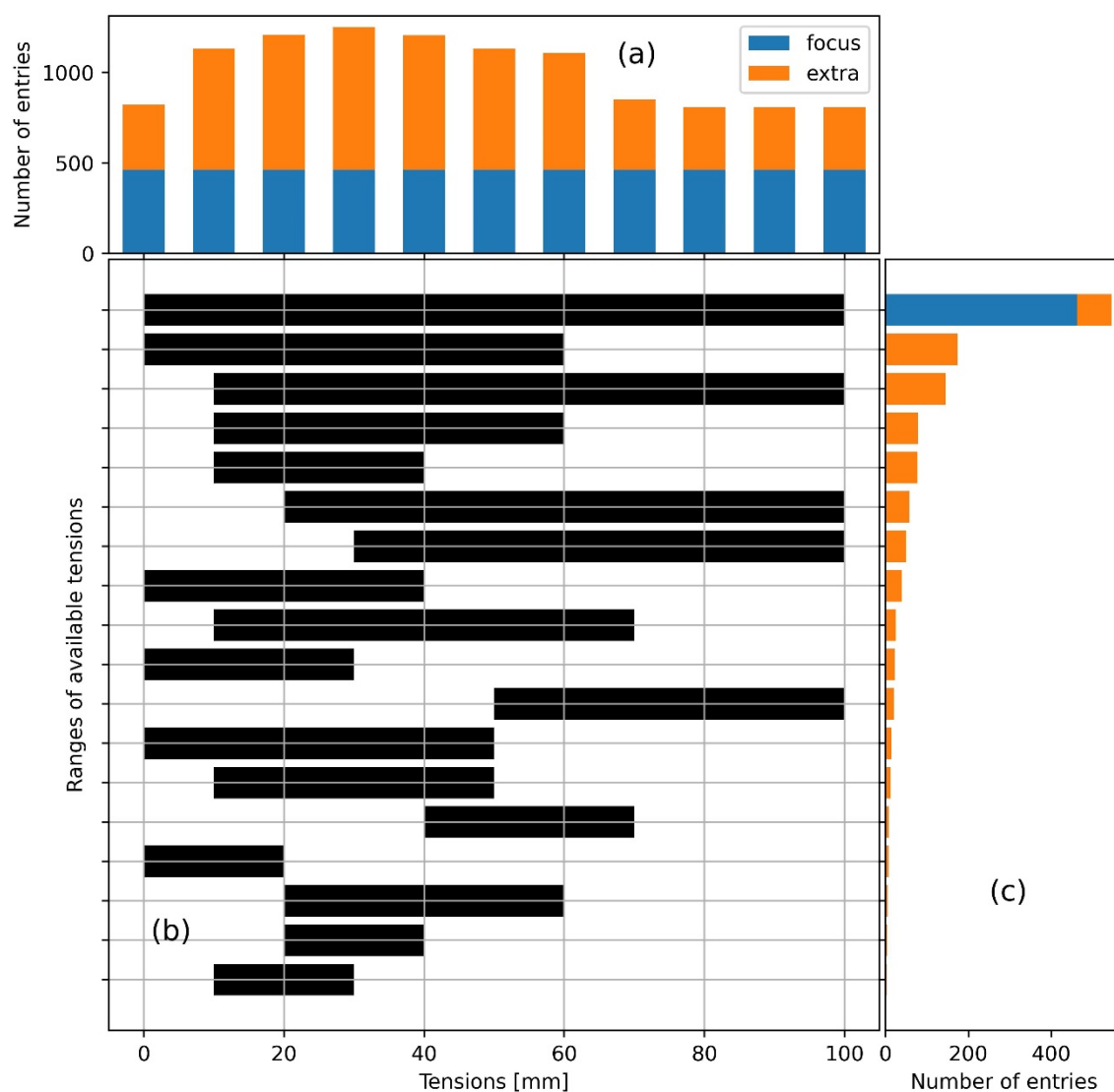
246 measured and reported in the source publications. A large number of entries span the full range of
 247 tensions of interest (0 to 100 mm), whereas a smaller number of entries only have data up to a tension
 248 of 60 mm. Often, but not always, such data series were obtained with the widely available Mini-Disk
 249 infiltrometer distributed by the *Meter* group (formerly by *Decagon*), which is limited to tensions $h \leq 70$
 250 mm. An overview on the metadata included in OTIM is given in Table 2. Data gaps are present,
 251 especially for bulk density and for information on the soil management at the study site, apart from
 252 tillage operations. Note that the annual mean temperature and precipitation are only two examples
 253 representing the climatic variables enumerated in section 2.3. There are very few missing values for
 254 the climate data, since it was estimated from the coordinates of the study sites. The same holds for the
 255 elevation data and information on the WRB soil type.

256 **Table 2: Number of entries and gaps for each feature along with units and range (if**
 257 **continuous) or choices (if categorical). The values are shown for the filtered entries**
 258 **(‘focus’) and in parenthesis for all the entries available in the database (‘focus’ and ‘extra’).**

Type	Predictor	Unit	Range/Choices	Number of entries	Number of gaps
Soil	Sand content	kg kg ⁻¹	0.0 -> 0.9 (0.0 -> 1.0)	402 (1070)	64 (215)
Soil	Silt content	kg kg ⁻¹	0.0 -> 0.8 (0.0 -> 0.8)	402 (1070)	64 (215)
Soil	Clay content	kg kg ⁻¹	0.0 -> 0.7 (0.0 -> 0.8)	405 (1107)	61 (178)
Soil	Bulk density	g cm ⁻³	0.5 -> 1.8 (0.1 -> 2.2)	324 (771)	142 (514)
Soil	Soil organic carbon	kg kg ⁻¹	0.0 -> 0.1 (0.0 -> 1.0)	339 (938)	127 (347)
Climate	Annual mean temperature	°C	-0.4 -> 29.1 (-3.8 -> 29.1)	466 (1214)	0 (71)
Climate	Annual mean precipitation	mm	22.0 -> 3183.0 (22.0 -> 3183.0)	466 (1214)	0 (71)
Climate	Average aridity index	-	0.0 -> 1.9 (0.0 -> 2.8)	466 (1214)	0 (71)
Climate	Precipitation seasonality (CV)	-	9.9 -> 138.5 (9.6 -> 138.5)	466 (1214)	0 (71)
Climate	Mean diurnal range	°C	6.9 -> 18.2 (4.8 -> 18.5)	466 (1214)	0 (71)

Management	Land use	-	arable, bare, grassland, woodland/plantation	453 (1249)	13 (36)
Management	Tillage	-	conventional tillage, no tillage, reduced tillage	422 (1190)	44 (95)
Management	Soil compaction	-	compacted, not compacted	76 (265)	390 (1020)
Management	Sampling time	-	soon after tillage, consolidated soil	367 (993)	99 (292)

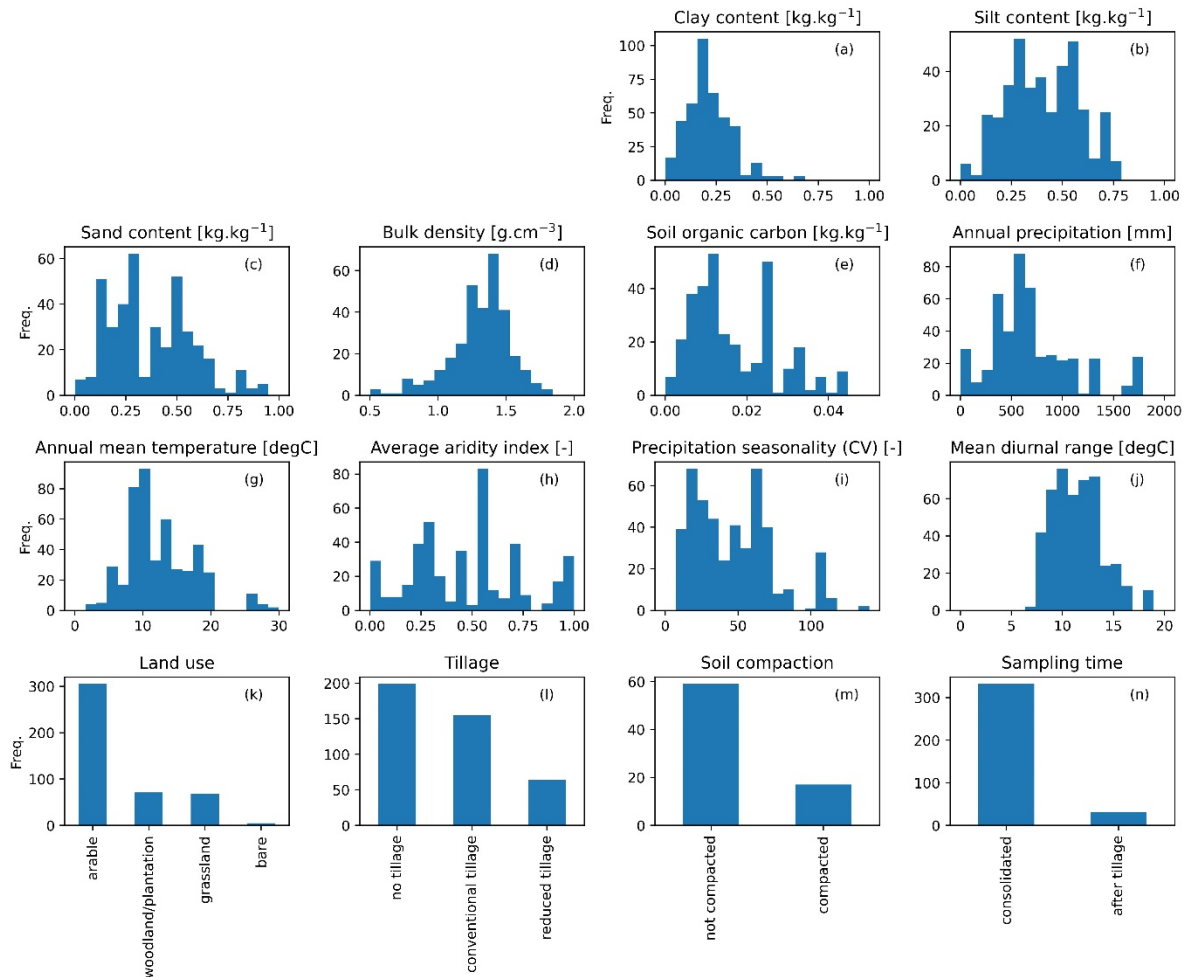
259



260

261 **Figure 3: (a) number of available K_h values per supply tension, (b) available tension series**
 262 **with the black bar indicating the span between T_{min} and T_{max} (c) their respective frequency**
 263 **in the database. The values are shown for the filtered entries ('focus') and for all the entries**
 264 **available in the database ('focus' and 'extra').**

265 The metadata for the datasets used in the exploratory data analysis are summarized in Figure 4. OTIM
 266 contains predominantly data from arable fields. The distributions of the climate variables confirms that
 267 the data in OTIM was also mostly acquired in temperate climates, with a bias towards the somewhat
 268 drier climates that are most typical for arable land. The soil texture, bulk density and organic carbon
 269 content data also appear reasonably representative for soils in this climate zone.



270

271 **Figure 4: Distributions of continuous and categorical variables in the ‘focus’ dataset.**

272 **2.3 Exploratory data analysis**

273 Some source publications only provided a few data entries for K_h , sometimes only comparing two
 274 different treatments, while other source studies contain data for a larger number of treatments and/or
 275 sites. In some publications, data for all individual tension-disk measurements are available, even if
 276 replicates were measured. In others, only averages of the replicated measurements are reported, while
 277 still others yield average K_h values for individual replicated treatment blocks. This makes appropriate
 278 data weighting complicated, but also extremely important when analysing the meta-dataset. It also
 279 introduces uncertainty, because it is not always clear whether the replicated averages were calculated
 280 using the geometric or the arithmetic mean. Considering that hydraulic conductivities at or near
 281 saturation are known to be log-normally distributed, the former would be best. In the following, we

282 assumed that geometric averaging was used when replicated values were reported in source
283 publications. In the following, we calculated data weights as

$$284 \quad \omega_i = \frac{n_{r,i}}{\sqrt{N_i}} \quad \text{Equation 1}$$

285 where ω_i is the weight for data entry i , $n_{r,i}$ is the number of replicates from which the values of i were
286 averaged and N_i is the total number of measurements included in the publication from which data entry
287 i was obtained. With this approach, we up-weighted data entries according to the number of replicate
288 measurements from which they were averaged and down-weighted the impact of studies that published
289 larger amounts of data.

290 We used weighted Spearman rank correlation coefficients to investigate relationships between
291 continuous variables. We considered correlations significant if they exhibited p-values of less than 0.05.
292 The latter were determined numerically by running randomization tests with 200 repetitions.

293 2.4 Meta-analysis

294 Data entries in OTIM with specific land use or management were very unevenly distributed. For
295 example, the large majority of data was measured on sites with land use 'arable' (see Figure 4a). Such
296 uneven distributions may lead to bias when averaged over all entries of a specific feature in exploratory
297 data analyses. We therefore investigated the effects of land use and management as well as soil
298 compaction and time of measurement on K_r with the aid of pairwise comparisons published within
299 individual studies and calculated effect sizes (ES) for each investigated class.

300 To reduce bias arising from the varying number of data entries published within individual studies, we
301 grouped all entries according to the factors land use, tillage, compaction, and sampling time. Here we
302 only considered binary pairs, that is arable or not arable in the case of land use and tilled or not tilled,
303 compacted or not compacted as well as 'measured soon after tillage' or 'measured on consolidated soil'
304 for the other three factors. In addition, we checked whether different entries within individual studies
305 stemmed from the same or a very similar site. We did this by comparing the respective USDA texture
306 classes and a climate variable, namely the aridity class. All data entries within each individual study that

307 exhibited identical land use, soil management, soil compaction, sampling time, texture and aridity were
 308 averaged and the number of corresponding replicates was summed.

309 For each binarized factor (e.g. tillage), a *control* value was chosen (e.g. zero tillage). All values different
 310 from the control represent the *treatment* (e.g. conventional tillage and reduced tillage). Within individual
 311 studies, pairs among the averaged entries were formed for each combination of a control and a
 312 treatment value. These pairs were used to compute the effect size. Following Basche and DeLonge
 313 (2019), we defined the effect sizes as the \log_{10} of the ratio of $K_{h,t}$ of the treatment divided by $K_{h,c}$ of the
 314 control

$$315 \quad ES_l = \log_{10} \left(\frac{K_{h,t}}{K_{h,c}} \right) \quad \text{Equation 2}$$

316 where the subscript l indicates the l^{th} pair for which the effect size was computed and the indices ‘ t ’ and
 317 ‘ c ’ stand for treatment and control, respectively. The average effect size ES for each of the four
 318 investigated factors was calculated as the weighted mean of the individual ES_l using the weight

$$319 \quad w_l = \frac{v_c v_t}{v_c + v_t} \quad \text{Equation 3}$$

320 where the subscript l indicates again the l^{th} pair for which the effect size was computed and v_c and v_t
 321 denote the number of (summed) replicates for control and treatment, respectively. In addition, we
 322 calculated the weighted standard error

$$323 \quad \sigma_{\overline{ES}} = \sqrt{\frac{\sum_{l=0}^n w_l (ES_l - \overline{ES})^2}{\frac{n-1}{n} \sum_{l=0}^n w_l}} \quad \text{Equation 4}$$

324 where \overline{ES} is the mean effect size. Table 3 summarises the evaluated factors, the number of pairs
 325 involved and the number of different studies from which the pairs were obtained.

326 To estimate the robustness of the effect size, we carried out a sensitivity analysis using the Jackknife
 327 technique, similarly to Basche and DeLonge, 2019. This method aims to show the sensitivity of the

328 averaged effect size to data from specific studies. For each factor, a given number of studies was
 329 randomly picked and removed from the dataset. The averaged effect size and its standard error were
 330 computed with the rest of the dataset. The process started by removing one study, after which up to
 331 nine more studies were removed. This random selection was repeated 50 times to rule out bias. The
 332 average of the means and standard errors for the 50 realisations was computed and plotted. Observed
 333 effect sizes were judged trustworthy if they did not change after removal of studies to calculate
 334 them. We constrained the sensitivity analyses in our study to the effect sizes for K_s and K_{100} .

335 **Table 3: Number of studies and paired comparison with their respective control and**
 336 **treatment values used for the meta-analysis exemplary for the K_{100} values.**

Factor	Control	Treatments	Studies	Paired comparisons
Land use	not arable	arable	10	24
Tillage	no tillage	conventional tillage, reduced tillage	15	32
Compaction	not compacted	compacted	6	8
Sampling Time	consolidated soil	soon after tillage	6	12

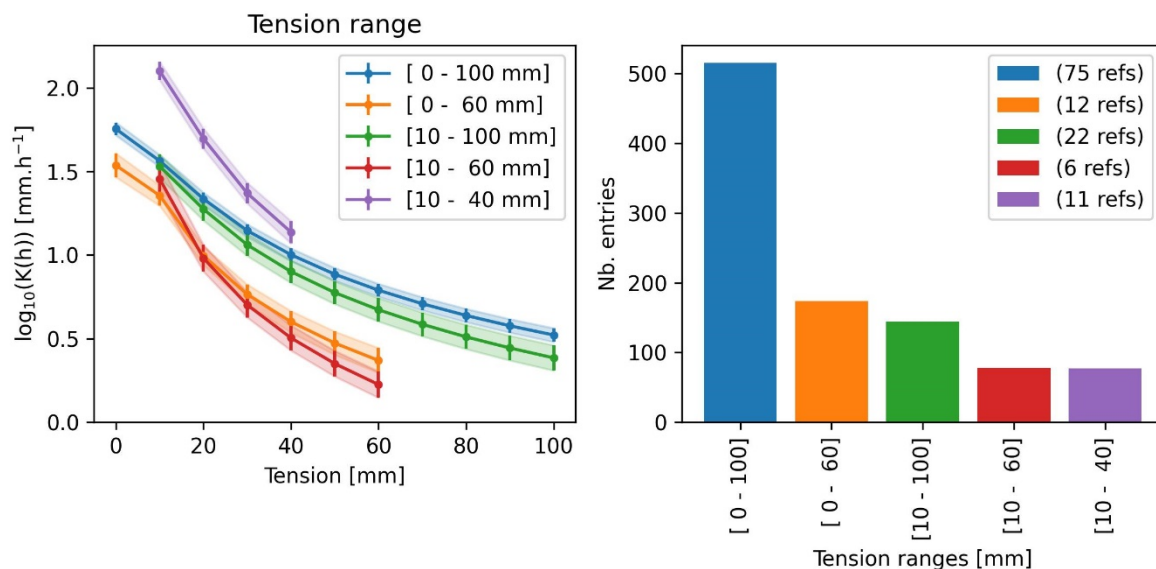
337

338 3 Results and discussion

339 3.1 Differences between data entries with different tension ranges

340 If all data are considered ('focus' and 'extra'), Figure 3 illustrates that approximately 40% of the data in
 341 OTIM provided K_h for every h with $0 \leq h \leq 100$ mm. For another 40%, K_h was only measured in the wet
 342 range, i.e. at tensions below 70 mm. The remaining K_h data was only acquired at the dry range. Here,
 343 we counted all data entries for which K_s were not measured and could not be estimated. Figure 5 shows

344 how data from entries with complete, dry and wet ranges differed. The K_h for the wet range receded
 345 faster with increasing tension than series that also included measurement in the dry range. A large
 346 portion of these datasets were obtained with the Mini-Disk infiltrometer. However, a closer inspection
 347 of the impact of the disk diameters used to acquire the respective K_h did not confirm suspicions that the
 348 bias was related to the use of this special type of infiltrometer (see Figure 6a). The observed differences
 349 between the K_h curves could have been introduced by co-correlations with soil texture or climate.
 350 Another explanation may be experimenter bias, since individual research groups tend to use specific
 351 tension ranges for more than one study. In this study, however, we focused solely on data entries for
 352 which we were able to reconstruct K_h for all h in between 0 and 100 mm supply tension in the following
 353 exploratory data analyses and meta-analyses. This greatly facilitated the data interpretation.



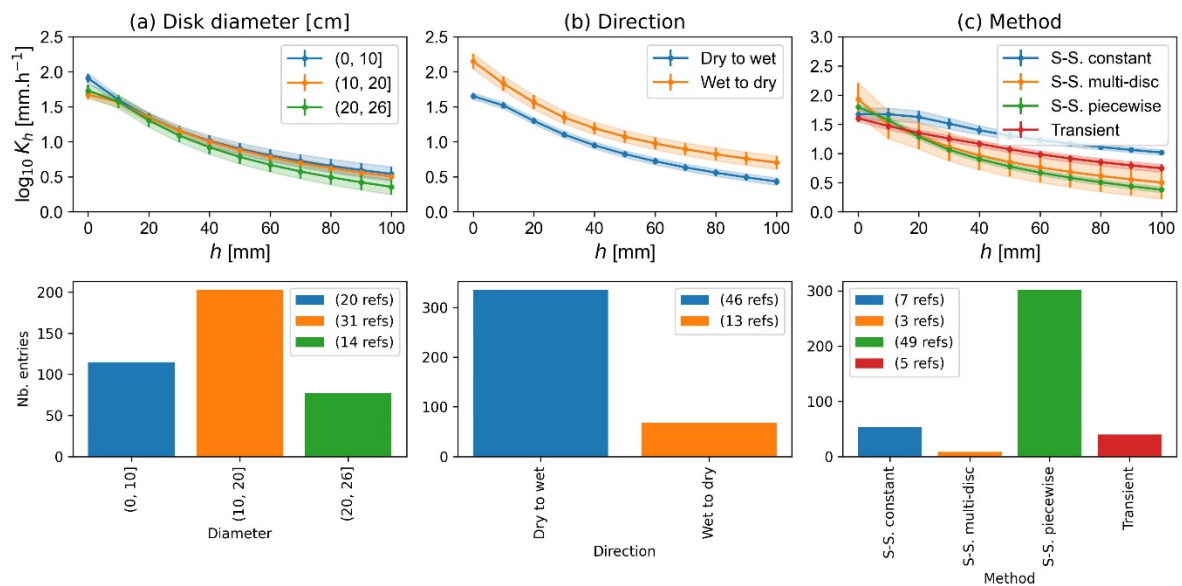
354

355 **Figure 5: Evolution of weighted mean K_h with tension available in OTIM, sorted by the**
 356 **tension range the data was spanning. The number of publications from which the data**
 357 **originated is shown between parentheses in the legend. The shaded areas and the error**
 358 **bars represent the weighted standard error of the mean.**

359 3.2 Statistical relationships between K_h and methods used

360 Figure 6a confirms that the diameter of the tension disk did not have a systematic impact on the results.
 361 The majority of the data were collected starting under dry conditions (large tensions) and subsequently
 362 measured under increasingly wet conditions (smaller tensions). Figure 6b illustrates that beginning the

363 experiment under wet conditions is associated with larger hydraulic conductivities at identical supply
 364 tensions. This is well known and is referred to as hysteresis, which is due to ink-bottle effects, impacts
 365 of water repellency, air entrapment and swelling of clay particles (Hillel, 2004). Figure 6c shows that the
 366 large majority of studies used the ‘steady-state piecewise’ method to solve the Wooding equation and
 367 convert the measured infiltration rates to hydraulic conductivities. This method leads to smaller K_h for
 368 larger tensions than the other methods. The ‘transient’ and ‘steady-state constant’ methods yielded
 369 larger K_h in the unsaturated range. For the latter method, it is known that it overestimates unsaturated
 370 K_h (Jarvis et al., 2013). We tested whether excluding data from ‘transient’ and ‘steady-state constant’
 371 methods changed the results of the meta-analyses, but found that they only changed to a minor degree.
 372 Data from all methods were therefore included in the following. Note that the ‘transient’ method was
 373 mostly applied in conjunction with Mini-Disk Infiltrometers, albeit the respective data is not included in
 374 Figure 6 since it does not span the entire suction range.

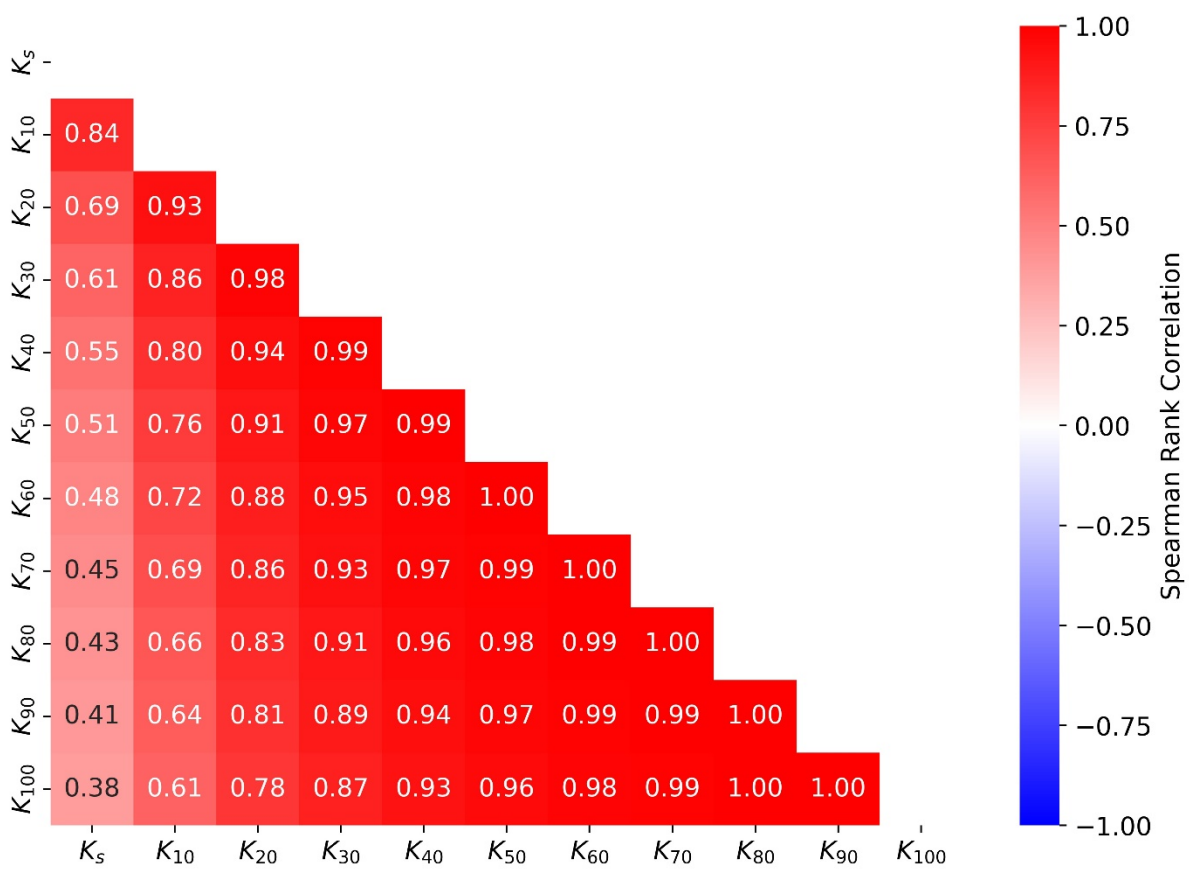


375

376 **Figure 6: Evolution of weighted mean K_h as a function of applied tension for (a) disk**
 377 **diameter, (b) direction and (c) method of fitting. ‘S.-S.’ stands for ‘steady-state’. More**
 378 **specifically, the method ‘S.-S. constant’ is outlined in Logsdon and Jaynes (1993), ‘S.-S.**
 379 **multi-disc’ in Smettem and Clothier (1989), and ‘S.-S. piece-wise’ in Reynolds and Elrick**
 380 **(1991) or Ankeny et al. (1991) and ‘Transient’ in Zhang (1997) or Vandervaere et al. (2000).**
 381 **The shaded areas and the error bars represent the weighted standard error of the**
 382 **mean. The bar plots in each subplot indicate how many data points of each class were in**
 383 **the data set.**

384 3.3 Correlation between K_h at different tensions

385 The fact that correlations between K_h estimated at supply tensions between 40 and 100 mm were
 386 relatively stable (Table 4) indicates that the respective flow paths and/or mechanisms remained very
 387 similar in this tension range. However, these correlations weakened at tensions between 10 and 20
 388 mm, giving rise to the existence of a threshold above which water flow in the largest macropores
 389 becomes the dominant flow mechanism. The poor correlation between K_s and K_h at larger supply
 390 tensions is in line with findings that K_s is not well suited to infer to soil unsaturated hydraulic
 391 conductivities (Schaap and Leij, 2000).



392

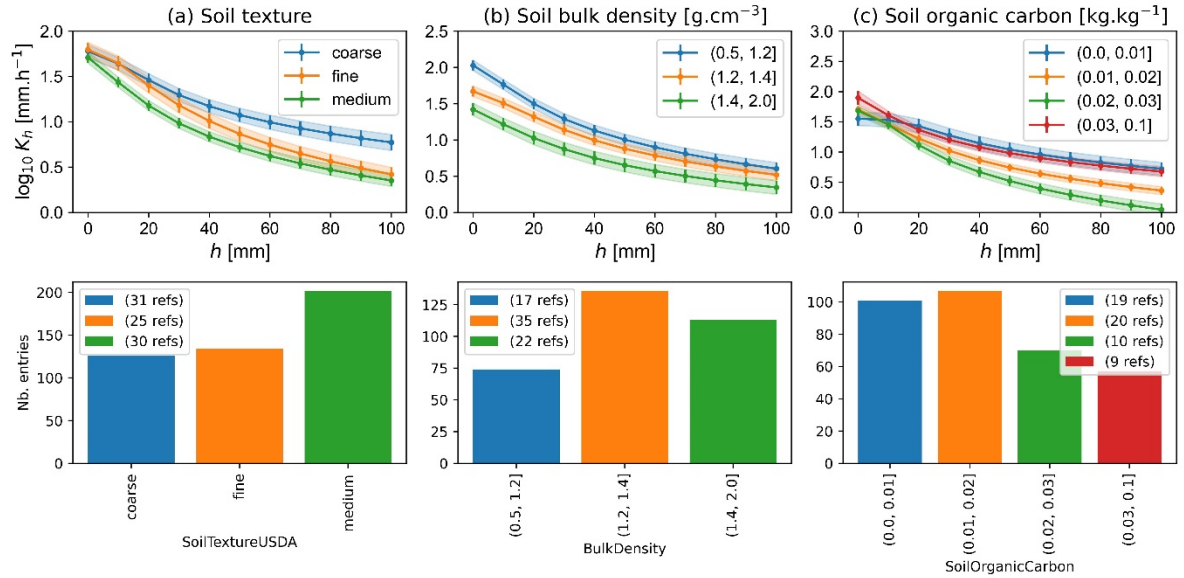
393 **Table 4: Weighted Spearman rank correlation coefficients between K_h at different tensions.**

394 **Correlation coefficients are shown up to p-values of 0.001.**

395 3.4 Statistical relationships between K_h and soil properties

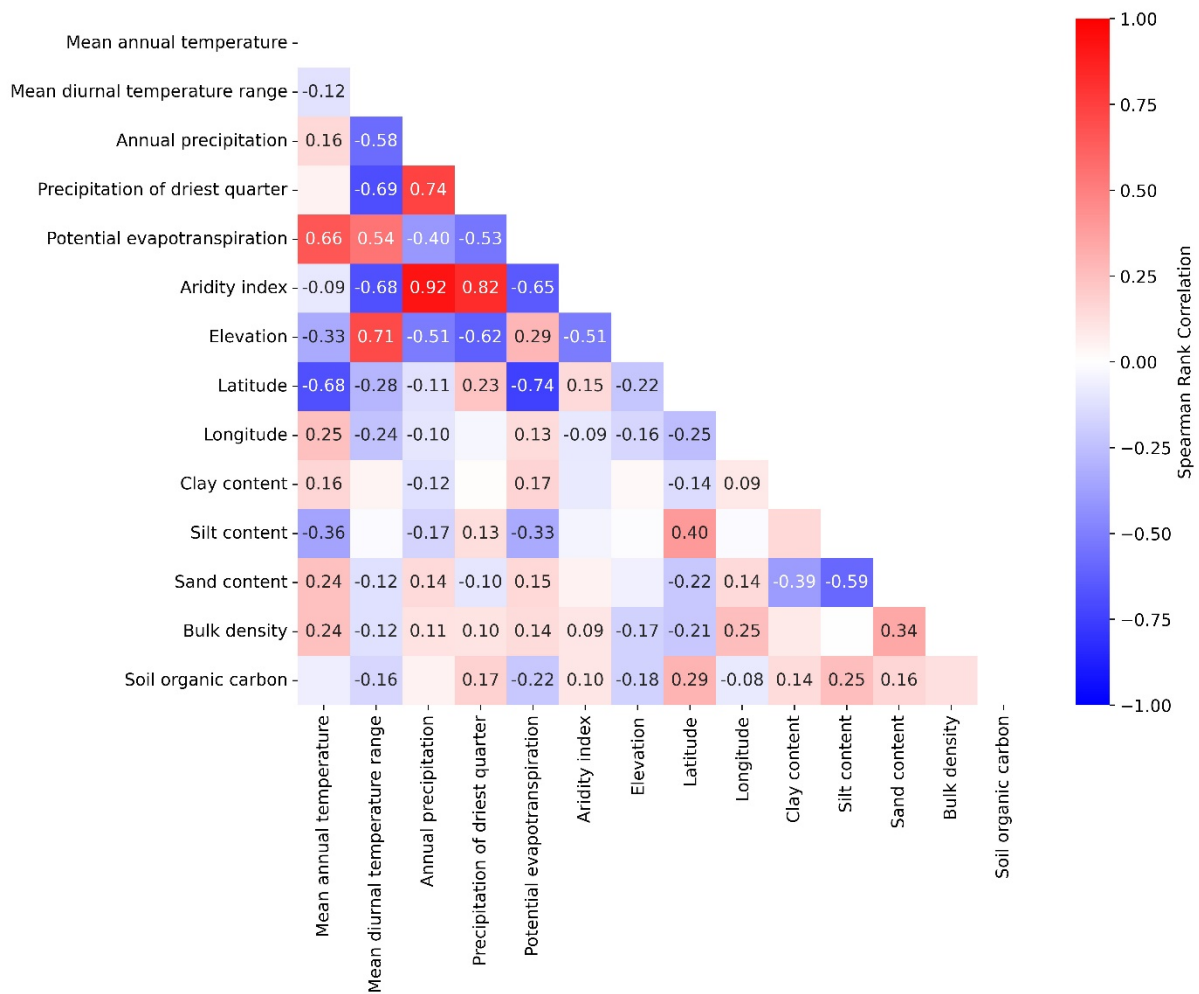
396 Soils with coarse texture exhibited larger K_h in the unsaturated range, which is caused by the large and
397 abundant primary pores in between individual sand grains (Figure 7a). At saturation, the average
398 hydraulic conductivity of all three texture classes was similar. This is explained by the presence of large
399 structural pores in the medium and fine-textured soils. Medium-textured soils had the lowest K_h in the
400 investigated range of tensions, which may be due to a denser soil matrix in loamy soils and a lower
401 structural stability of silty soils. Larger bulk densities decreased K_h across the whole range of
402 investigated tensions, which reflects the reduced porosity with increasing bulk density (Figure 7b).

403 The hydraulic conductivity in the saturated and near-saturated range is especially affected by soil
404 compaction, which predominantly reduces the abundance and connectivity of macropores (Pagliai et
405 al., 2004; Whalley et al., 1995). Large bulk densities are also known to reduce burrowing activities of
406 the soil macrofauna (Capowiez et al., 2021) as well as root growth (Lipiec and Hatano, 2003), also
407 leading to less abundant and less connected large macropores. An increase in the soil organic carbon
408 content was connected with smaller K_h at the dry end of the investigated tension range if soils with
409 organic carbon contents of more than 0.03 kg.kg⁻¹ were excluded (Figure 7c). This decrease may be
410 explained by water repellency, which is generally positively correlated with organic carbon content. A
411 similar observation was already reported in Jarvis et al. (2013). Note that no major correlations of SOC
412 with soil texture were observed in the investigated dataset (Table 5). For soils with organic carbon
413 contents larger than 0.03 kg.kg⁻¹, K_h increased once again. This may indicate that, above this threshold,
414 better-developed macropore networks associated with large SOC contents (e.g. Larsbo et al., 2016b)
415 outweighed any effects of water repellency.



416

417 **Figure 7: Evolution of weighted mean K_h as a function of applied tension for (a) soil texture,**
 418 **(b) soil bulk density and (c) soil organic carbon. The shaded areas and the error bars**
 419 **represent the weighted standard error of the mean. The soil textures were classified using**
 420 **USDA texture classes as follows: fine (clay, clay loam, silty clay, silty clay loam), medium**
 421 **(silt loam, loam), coarse (loamy sand, sand, sandy clay, sandy clay loam, sandy loam). The**
 422 **bar plots in each subplot indicate how many data points of each class were in the data set.**



423

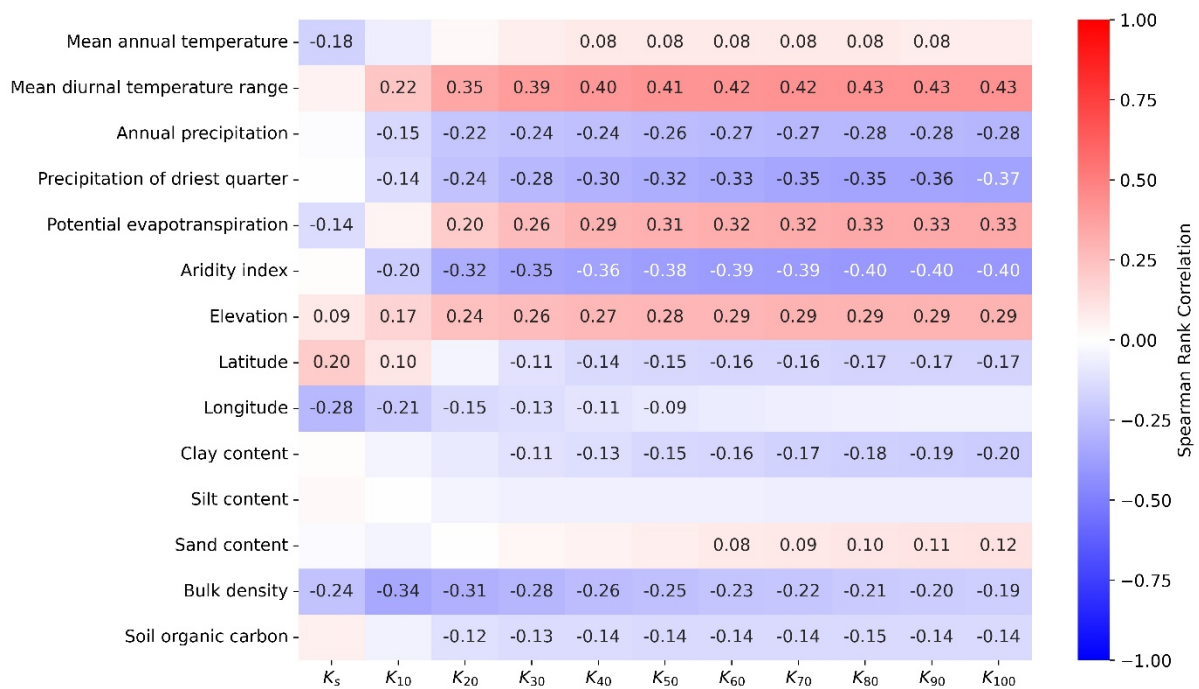
424 **Table 5: Weighted Spearman rank correlation coefficients between climate variables,**
 425 **elevation above sea level and soil properties. Correlation coefficients are shown up to p-**
 426 **values of 0.001.**

427 **3.5 Statistical relationships between K_h and climate variables**

428 One important observation made in recent years was that saturated and near-saturated hydraulic
 429 conductivities correlated strongly with climate variables (Jarvis et al., 2013; Jorda et al., 2015; Hirmas
 430 et al., 2018). Table 6 gives an overview of weighted Spearman rank correlations between K_h and six of
 431 the 20 climate variables included in OTIM that exhibited the strongest correlations with K_h . The elevation
 432 of the sampling site above sea level, its latitude and longitude, soil texture, bulk density and soil organic
 433 carbon content are also shown for comparison. It is striking that the soil properties were less well
 434 correlated with K_h than some of the climate variables. Of the three USDA texture fractions, the clay
 435 content was negatively and the sand content positively correlated with K_h at the drier investigated

436 tension range, while no significant correlations were found for the silt fraction (Table 6). Only the bulk
 437 density exhibited correlation coefficients as large as the climate variables.

438 The largest absolute values of the weighted rank correlations were observed for the mean diurnal range
 439 of temperature and the aridity index. Both reach a maximum at the dry end of the considered tension
 440 range, i.e. for K_{100} , with correlation coefficients of 0.43 and -0.4, respectively. Table 5 reveals that both
 441 of these best correlated climate variables were accidentally correlated with choices in experimental
 442 design and data evaluation made by the investigators in the respective source studies that will amplify
 443 these observed correlations to K_h . However, if a smaller dataset is considered in which such
 444 methodological bias as well as potential bias due to differences in land use were eliminated, the
 445 correlations persisted (Table B1). We therefore infer that the observed effect of climate on K_h is real.



446

447 **Table 6: Weighted Spearman rank correlation coefficients between K_h at different tensions**
 448 **and climatic features and soil properties. Correlation coefficients are shown up to p-values**
 449 **of 0.001.**

450 The annual mean diurnal temperature range and the aridity index were strongly correlated with each
451 other, with a weighted correlation coefficient of -0.68 (Table 5). Strong correlations to at least one of
452 these two variables with absolute values >0.6 were also found for most of the investigated climate
453 variables. It is therefore difficult to separate the climate effects due to these strong inter-correlations.
454 Nevertheless, it is striking that the mean annual diurnal temperature ranges are much better correlated
455 with K_{100} than the mean annual temperature itself (Table 6). In addition, the mean annual precipitation
456 in the driest quarter of the year and the precipitation in the driest quarter of the year exhibited stronger
457 correlations than the mean annual precipitation. It appears that temperature and precipitation
458 fluctuations are more strongly coupled to near-saturated hydraulic conductivities than the absolute
459 temperatures or precipitation amounts.

460 Among possible reasons for the observed correlations may be increased splash erosion during heavy
461 rainfalls that are common in regions with large precipitation seasonality, more soil compaction in wetter
462 climates due to trafficking, a larger vertical burrowing activity of soil fauna in climates with large diurnal
463 temperature ranges, more vertically oriented root systems in arid climates or climate specific choices in
464 land use and soil management. The data in OTIM cannot provide an answer to these questions.
465 Investigations of such relationships should be the focus of future studies.

466 Another site factor that is positively correlated with K_h is the elevation above sea level (Table 6). Notably,
467 elevation above sea level also was found to be an important predictor for K_s in Gupta et al. (2021b),
468 which suggests that there are indeed pedogenetic reasons behind the observed correlation. In the case
469 of infiltrometer measurements, the decreased atmospheric pressure with height on the supply tension
470 can be neglected. The supply tension is always equivalent to the weight of the water column adjusted
471 in the bubbling tower. The weight of the water column will be smaller due to the general decrease of
472 earth's gravitational constant with height due to a larger centrifugal force. However, the weight of the
473 water column would only be reduced by approximately one or two percent. Also, indirect influences of
474 larger heights on the infiltration rate cannot explain the observed correlation. A lower temperature would
475 make the water column denser. However, the effect would be less than 1% in the relevant temperature
476 range. In contrast, a lower temperature would increase the viscosity of water to a much larger degree,

477 e.g. by up to approximately 30% between temperatures of 10 and 20 °C. The temperature effect should
478 thus lead to a negative correlation between elevation and K_h , which is the opposite of what was
479 observed. Bias in the K_h measurements due to such physical effects can thus be ruled out. Elevation
480 may instead be a proxy for well-drained soils, as stagnant soil water and high groundwater tables are
481 less likely with height above sea level. This may favour soil life and better developed root systems and
482 decrease risks of compaction when the soil is trafficked.

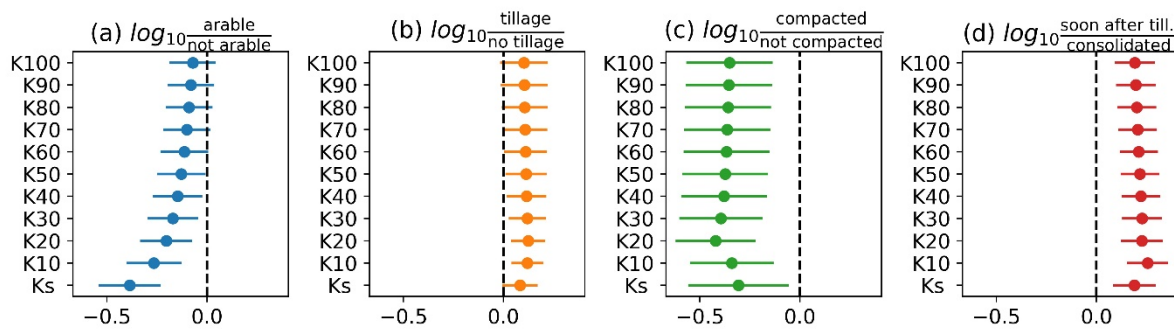
483 The observed correlations of K_h with latitude and longitude probably reflect co-correlations with climate
484 variables together with experimenter bias, since it appears likely that approaches in setting up tension
485 disk infiltrometers systematically vary between continents, e.g. America and Europe.

486 Bulk density was the only soil property that exhibited (negative) correlation strength of > 0.3 to any K_h
487 (Table 6). The underlying reasons have been discussed above. Notably, the strongest correlations were
488 found at and very close to saturation, probably due to the detrimental effect of soil compaction on
489 macroporosity and macropore connectivity. The more compaction, the less macroporosity remains and
490 the higher the bulk density, which in turn decreases root growth and bioturbation (Capowiez et al., 2021;
491 Lipiec and Hatano, 2003). The only pedo-climatic factor with relatively larger correlation strength (-0.31)
492 with the saturated hydraulic conductivity was the bulk density (Table 6).

493 3.6 Effects of land use, tillage, compaction and sampling time

494 The average \log_{10} response ratios shown in Figure 8 illustrate the effects of land use and soil
495 management on K_h for $0 \leq h \leq 100$ mm. Note that a value of ± 0.3 in the \log_{10} response ratio corresponds
496 to a factor 2. Hence, K_s for uncompacted soil was found to be approximately twice as large as for
497 compacted soil (see Figure 8c). Arable land exhibited clearly smaller K_s than grasslands and forests,
498 which is in line with observations made by Basche and DeLonge, 2019. This difference became smaller
499 with higher tensions (Figure 8a). The large difference in K_h close to saturation was likely related to traffic
500 compaction as well as tillage operations that were applied to the majority of the investigated arable
501 soils, which lead to the destruction of connected biopores and hence a reduced K_s . On the other hand,
502 tillage breaks up intact soil into individual soil aggregates, which creates, at least initially, a well-
503 connected network of inter-aggregate pores that increase K_h in the near-saturated range (Sandin et al.,

2017; Schlüter et al., 2020). This effect of tillage can explain why near-saturated K_h under conventional and reduced tillage was larger than under no-till (Figure 8b). However, in this case, even K_s was larger in the tilled fields. It is likely that K_s was reduced in the no-till treatments due to traffic compaction on the fields and a lack of soil loosening by tillage as compared to conventionally tilled treatments. Note however, that we only investigated topsoils in this study. It is not clear that how different tillage types affect K_h in the subsoil. The impact of soil compaction on K_h was clearly negative in the entire investigated range of tensions (Figure 8c), which is explained by the reduction of porosity, and especially the macroporosity during compaction (see also Figure 7b). In contrast, if the K_h measurements were carried out shortly after tillage operations, K_h was increased for all investigated tensions, especially very close to saturation (Figure 8d). This confirms that tillage initially increases K_s , but that subsequent soil consolidation preferentially disconnects the largest macropores. As a consequence, K_h at and very close to saturation is reduced more strongly than K_h for higher tensions.

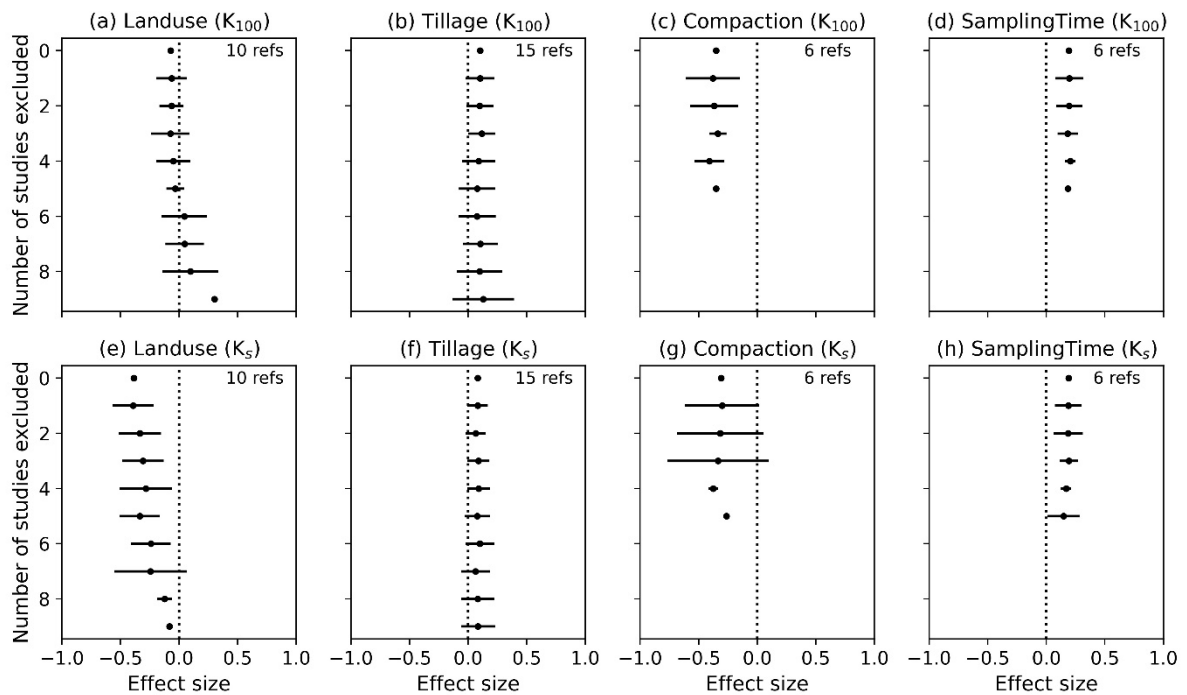


516

517 **Figure 8: Weighted mean \log_{10} response ratio (effect size) of K_h for from K_{100} to K_s for**
 518 **different management practises where the controls were ‘not arable’, ‘no tillage’, ‘no**
 519 **compaction’ and ‘consolidated soil’ respectively. Positive effect size means that the value**
 520 **of the treatment is greater than the control. Dashed line shows the “no effect” (no**
 521 **difference between treatment and control). Error bars represent the weighted standard**
 522 **error of the mean.**

523 Figure 9 shows the results of the sensitivity analyses for the effect sizes depicted in Figure 8. The effect
 524 of land use for K_{100} turned out to be the most sensitive to the removal of studies (Figure 9a). The
 525 direction of the effect even changed after removal of six studies, indicating that higher K_{100} for arable
 526 compared to non-arable fields were not just occasional observations but occurred more frequently. More
 527 studies would be needed to properly characterise the effect of land use on K_{100} . The remaining

528 sensitivity analyses for all the other factors showed that removal of studies did not change or destabilise
 529 the results for both K_{100} and K_s .

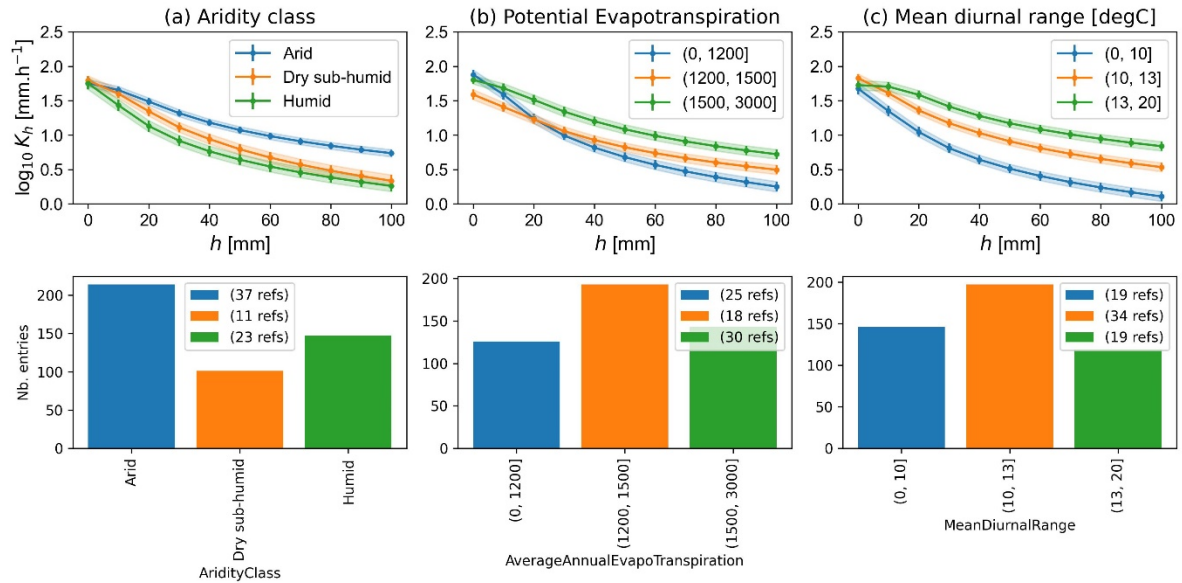


530

531 **Figure 9: Sensitivity analysis of the weighted effect size of K at 100 mm tension and K_s for**
 532 **the management practice investigated using the Jackknife technique. The error bars**
 533 **represent the standard error.**

534 **3.7 Comparison of effect size of land use and management and sampling time with**
 535 **effect of climate and soil properties**

536 Effect sizes could only be computed for land use and management, compaction as well as sampling
 537 time. It is therefore difficult to relate the impact of these factors to the ones of measurement method,
 538 climate variables and soil properties. Comparisons between figures 6, 7 and 10, on the one hand, with
 539 Figure 8 provide some insight. Land use and management related effects and sampling time (Figure 8)
 540 seem to have a similar effect on K_h as soil properties (Figure 7) and measurement method (Figure 6).
 541 Climate variables seem to have a larger impact on K_h at the dry end of the investigated tension range,
 542 but a smaller one close to saturation (Figure 10).



543

544 **Figure 10: Evolution of weighted mean K_h as a function of applied tension for (a) aridity**
 545 **class, (b) potential annual evapotranspiration and (c) mean annual diurnal temperature**
 546 **range. The shaded areas and the error bars represent the weighted standard error of the**
 547 **mean.**

548 4 Conclusions

549 Our results suggest that climate change will influence soil hydraulic properties near saturation. This
 550 may complicate model predictions of water balance in a future climate, particularly the risks of surface
 551 runoff, soil erosion and waterlogging. Climatic factors are more strongly correlated to near-saturated
 552 hydraulic conductivities than soil texture, bulk density and organic carbon content. At and very close to
 553 soil saturation, the correlations between hydraulic conductivity and climate variables vanished,
 554 indicating a change in flow paths. Instead, the soil bulk density showed the largest correlation, in line
 555 with the fact that more compact soils tend to lack a well-connected macropore system. Hypotheses as
 556 to why climate variables are correlated with the hydraulic conductivity were discussed, but these need
 557 to be further investigated. Most probably, the impacts of climate are linked to macropore networks
 558 associated with biological activity, pedogenesis, and land use. Only a few land use and soil
 559 management related factors could be investigated in our study. They were all found to significantly

560 influence K_h , with effect sizes similar to those of soil properties like texture and organic carbon content.
 561 Also, experimenter bias as introduced by choice of measurement time relative to soil tillage,
 562 experimental design or data evaluation appeared to be as important for the saturated and near-
 563 saturated hydraulic conductivity as soil texture or bulk density. There is a need for better documentation
 564 and accessibility of measurement data and associated meta-data, as has already been suggested by
 565 others (McBratney et al., 2011; Basche and DeLonge, 2019). OTIM offers the possibility to derive more
 566 comprehensive pedotransfer approaches than the ones in Jorda et al., (2015). The construction and
 567 evaluation of such pedotransfer functions is envisioned for an upcoming companion paper to this study.

568 5 Appendix A

569 5.1 Data query details

570 **Table A1: Query strings, search engines, number of result pages that were processed and**
 571 **dates of the search for finding new data for OTIM**

Search engine	Query string (time range considered)	Date	Pages
Google Scholar	hydraulic unsaturated conductivity tillage crop	2021/06/02	12
Google Scholar	tension disk infiltrometer	2021/06/02	3
Web of Science	field unsaturated hydraulic conductivity agriculture	2021/06/02	3
Google Scholar	Near-saturated hydraulic conductivity (2013-2021)	2021/06/01	~8
ISI Web	Near-saturated hydraulic conductivity (2013-2021)	2021/06/01	~8
Scopus	Near-saturated hydraulic conductivity (2013-2021)	2021/06/01	~8
Google Scholar	hydraulic conductivity (2013-2021)	2021/05/31	~8
ISI Web	hydraulic conductivity (2013-2021)	2021/05/31	~8
Scopus	hydraulic conductivity (2013-2021)	2021/05/31	~8
Google Scholar	tension disk infiltrometer (2013-2021)	2021/05/31	~5
ISI Web	tension disk infiltrometer (2013-2021)	2021/05/31	~5
Google Scholar	Near-saturated hydraulic conductivity (2013-2021)	10/06/2021	~8
Google Scholar	tillage hydraulic conductivity (2013-2021)	10/06/2021	~8
Google Scholar	tension disk infiltrometer tillage (2013-2021)	10/06/2021	~8
Scopus	Near-saturated hydraulic conductivity (2013-2021)	10/06/2021	~3
Scopus	tillage hydraulic conductivity (2013-2021)	10/06/2021	~3
Scopus	tension disk infiltrometer (tillage) (2013-2021)	10/06/2021	~3
Scopus	"near-saturated" and infiltration	18/06/2021	~4
Scopus	"mini disk infiltrometer"	18/06/2021	~4
Scopus	"tension infiltrometer"	23/06/2021	~5

572

573 5.2 Data rejection

574 **Table A2: Reasons for data rejection.**

Reason	Number of publications
no access	2
not relevant	19
only one tension	61
overlap with another paper	3
no data published	32

575

576 5.3 Database organisation

577 OTIM is organised in nine individual tables illustrated in Table A3. The main table is named *experiments*.

578 It contains identifiers with which all the other tables are linked. The identifiers are shown in bold font in

579 Table A3. The *reference* table contains information on the references for each study. The *location* table

580 lists the coordinates of the measurement sites. The tables *soilProperties*, *soilManagement* and *climate*

581 store data as implied by their names. The *method* table gives details on the specifications of the tension-

582 disk infiltrometer and the method to calculate hydraulic conductivity from the infiltration rate. The

583 *rawData* table contains the hydraulic conductivities and respective supply tensions as stated in the

584 corresponding source publication. Note that OTIM does not contain raw data for the entries of the

585 original version compiled for Jarvis et al., 2013. Finally, *modelFit* reports K_h for $0 \leq h \leq 100$ mm as

586 described above. For more details, the reader is directed to the 'description' tab of the database (not

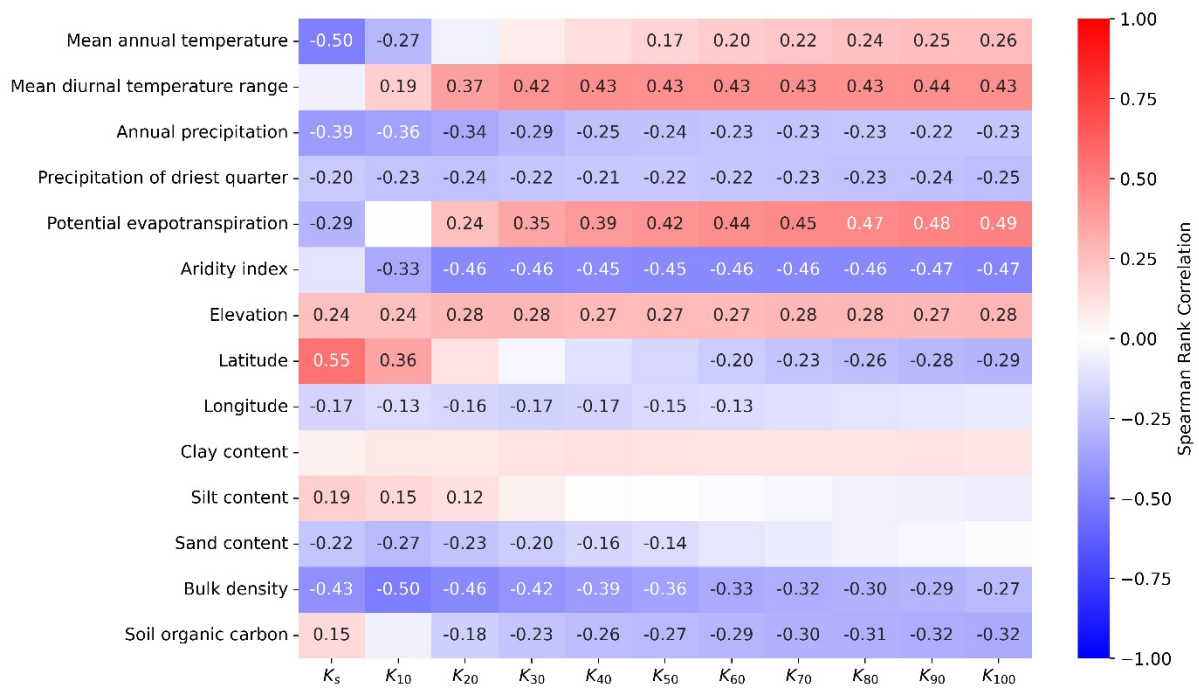
587 shown in Table A3) where the meanings and units of each column are explained.

locations	experiments	method	soilProperties
<ul style="list-style-type: none"> - LocID - Location - Latitude - Longitude - Comments 	<ul style="list-style-type: none"> - ExpID - ExpName - ReferenceTag - Location - ClimateName - MethodName - MTFName - SPName - SMName - DatasetAddedBy - DatasetCheckedBy 	<ul style="list-style-type: none"> - MTFID - MethodName - Month1 - Month2 - Season - Reps - YearExp - Method - Direction - Tmin - Tmax - UpperD_m - Diameter - Diameter2 - Diameter3 - Comment 	<ul style="list-style-type: none"> - SSPID - SPName - TextureClass - SoilTextureUSDA - SoilTextureFAO - SoilType - SoilTypeClass - ClayContent - SiltContent - SandContent - BulkDensity - SoilOrganicCarbon
climate	reference	modelFit	soilManagement
<ul style="list-style-type: none"> - ClimateName - AnnualMeanTemperature - MeanTemperatureofWarmestQuarter - MeanTemperatureofColdestQuarter - AnnualPrecipitation - PrecipitationofWettestMonth - PrecipitationofDriestMonth - PrecipitationSeasonality - PrecipitationofWettestQuarter - PrecipitationofDriestQuarter - PrecipitationofWarmestQuarter - PrecipitationofColdestQuarter - MeanDiurnalRange - Isothermality - TemperatureSeasonality - MaxTemperatureofWarmestMonth - MinTemperatureofColdestMonth - TemperatureAnnualRange - MeanTemperatureofWettestQuarter - MeanTemperatureofDriestQuarter - elevation - AverageAridityIndex - AverageAnnualEvapoTranspiration - AridityClass 	<ul style="list-style-type: none"> - RefID - ReferenceTag - ReferenceYear - ReferenceName - ReferenceDOI - ReferenceTitle - Comments 	<ul style="list-style-type: none"> - MTFName - K5 - Kunsat - slope - R2 - Hmin - intercept - K1 - K2 - K3 - K4 - K5 - K6 - K7 - K8 - K9 - K10 	<ul style="list-style-type: none"> - SMName - Landuse - LanduseClass - Tillage - TillageClass - NbOfCropRotation - CurrentCrop - CropClass - CropRotation - CoverCrop - CoverCropClass - Residue - ResidueClass - Grazing - GrazingClass - Irrigation - IrrigationClass - Compaction - CompactionClass - OtherAmendments - AmendmentClass - SamplingTime - SamplingTimeClass - Comments
rawData			
<ul style="list-style-type: none"> - MTFID - MTFName - h - Kunsat - units reported - Kunsat - n - comment 			

588

589 **Table A3: Structure of the OTIM database with its different tables and columns. In the**
590 ***soilManagement* table, the columns with the suffix “Class” denote columns in which the**
591 **data reported in the source publications were summarised into classes to facilitate**
592 **comparing them. For example, the reported *CurrentCrop* like wheat, rye, barley or oat was**
593 **assigned the *CropClass* cereals. The rows in bold denote unique identifiers with which the**
594 **table entries are linked to the *experiments* table.**

595 6 Appendix B



596

597 **Table B1: Weighted Spearman rank correlation coefficients between K_h at different**
 598 **tensions and climatic features, soil properties, land use and management factors and**
 599 **methodological details. In contrast to Table 6, only the 193 data entries from arable fields**
 600 **using a dry-to-wet sequence and the steady-state piecewise method (Reynolds and Elrick,**
 601 **1991; Ankeny et al., 1991) were considered. Correlation coefficients are shown up to p-**
 602 **values of 0.001.**

603 7 Code availability

604 All scripts used to compile this study are publically available in form of Jupyter notebooks on GitHub:
 605 <https://github.com/climasoma/OTIM> and <https://github.com/climasoma/machine-learning>.

606 8 Data availability

607 The OTIM database is available from the BONARES data repository
 608 <https://tools.bonares.de/doi/datasets>.

609 9 Author contribution

610 Funding acquisition: JK, SG; project administration, supervision and conceptualization: JK; meta-
611 database collation and validation: LA, GuBl, JK; Python code development, including visualization:
612 GuBl, JK; applying statistical analyses and writing original manuscript draft: GuBl, JK; Reviewing and
613 editing the manuscript: JK, NJ, SG; GiBr, GuBl.

614 10 Competing interests

615 11 The authors declare that they have no conflict of interest.

616 12 Acknowledgements

617 This study was carried out in the framework of the EJP Soil ClimaSoMa project, which has received
618 funding from the EU Horizon 2020 Research and Innovation programme under grant number 862695.
619 We thank Lionel Alletto, Mats Larsbo, Ali Meshgi and Wim Cornelis for sharing additional details to their
620 source publication.

621 13 References

- 622 Alagna, V., Bagarello, V., Di Prima, S., and Iovino, M.: Determining hydraulic properties of a loam soil
623 by alternative infiltrometer techniques: Hydraulic Properties of a Loam Soil by Infiltration Techniques,
624 *Hydrol. Process.*, 30, 263–275, <https://doi.org/10.1002/hyp.10607>, 2016.
- 625 Alletto, L., Pot, V., Giuliano, S., Costes, M., Perdrieux, F., and Justes, E.: Temporal variation in soil
626 physical properties improves the water dynamics modeling in a conventionally-tilled soil, *Geoderma*,
627 243–244, 18–28, <https://doi.org/10.1016/j.geoderma.2014.12.006>, 2015.
- 628 Angulo-Jaramillo, R., Vandervaere, J. P., Roulier, S., Thony, J. L., Gaudet, J. P., and Vauclin, M.: Field
629 measurement of soil surface hydraulic properties by disc and ring infiltrometers - A review and recent
630 developments, *Soil Tillage Res.*, 55, 1–29, 2000.

631 Ankeny, M. D., Ahmed, M., Kaspar, T. C., and Horton, R.: Simple field method for determining
632 unsaturated hydraulic conductivity, 55, 467–470, 1991.

633 Bagarello, V., Baiamonte, G., Castellini, M., Di Prima, S., and Iovino, M.: A comparison between the
634 single ring pressure infiltrometer and simplified falling head techniques: COMPARING PRESSURE
635 INFILTROMETER AND SFH TECHNIQUES, *Hydrol. Process.*, 28, 4843–4853,
636 <https://doi.org/10.1002/hyp.9980>, 2014.

637 Baranian Kabir, E., Bashari, H., Bassiri, M., and Mosaddeghi, M. R.: Effects of land-use/cover change
638 on soil hydraulic properties and pore characteristics in a semi-arid region of central Iran, *Soil and Tillage
639 Research*, 197, 104478, <https://doi.org/10.1016/j.still.2019.104478>, 2020.

640 Basche, A. D. and DeLonge, M. S.: Comparing infiltration rates in soils managed with conventional and
641 alternative farming methods: A meta-analysis, 14, <https://doi.org/10.1371/journal.pone.0215702>, 2019.

642 Bártková, K., Miháliková, M., and Matula, S.: Hydraulic Properties of a Cultivated Soil in Temperate
643 Continental Climate Determined by Mini Disk Infiltrometer, *Water*, 12, 843,
644 <https://doi.org/10.3390/w12030843>, 2020.

645 Bodner, G., Scholl, P., Loiskandl, W., and Kaul, H. P.: Environmental and management influences on
646 temporal variability of near saturated soil hydraulic properties, 204, 120–129,
647 <https://doi.org/10.1016/j.geoderma.2013.04.015>, 2013.

648 Bottinelli, N., Menasseri-Aubry, S., Cluzeau, D., and Hallaire, V.: Response of soil structure and
649 hydraulic conductivity to reduced tillage and animal manure in a temperate loamy soil, *Soil Use Manage*,
650 29, 401–409, <https://doi.org/10.1111/sum.12049>, 2013.

651 Bouma, J.: Using soil survey data for quantitative land evaluation, 9, 177–213, 1989.

652 Capowiez, Y., Sammartino, S., Keller, T., and Bottinelli, N.: Decreased burrowing activity of endogeic
653 earthworms and effects on water infiltration in response to an increase in soil bulk density, *Pedobiologia*,
654 85-86, 150728, 2021.

655 Costa, J. L., Aparicio, V., and Cerdà, A.: Soil physical quality changes under different management
656 systems after 10 years in the Argentine humid pampa, *Solid Earth*, 6, 361–371,
657 <https://doi.org/10.5194/se-6-361-2015>, 2015.

658 De Boever, M., Gabriels, D., Ouessar, M., and Cornelis, W.: Influence of Acacia Trees on Near-Surface
659 Soil Hydraulic Properties in Arid Tunisia, *Land Degrad. Develop.*, 27, 1805–1812,
660 <https://doi.org/10.1002/ldr.2302>, 2016.

661 Etana, A., Larsbo, M., Keller, T., Arvidsson, J., Schjønning, P., Forkman, J., and Jarvis, N.: Persistent
662 subsoil compaction and its effects on preferential flow patterns in a loamy till soil, *Geoderma*, 192, 430–
663 436, <https://doi.org/10.1016/j.geoderma.2012.08.015>, 2013.

664 Fashi, F. H., Gorji, M., and Sharifi, F.: THE USE OF SOIL HYDRAULIC PROPERTIES AS
665 INDICATORS FOR ASSESSING THE IMPACT OF MANAGEMENT PRACTICES UNDER SEMI-ARID
666 CLIMATES, *Environ. Eng. Manag. J.*, 18, 1057–1066, <https://doi.org/10.30638/eemj.2019.102>, 2019.

667 Fasinmirin, J. T., Olorunfemi, I. E., and Olakuleyin, F.: Strength and hydraulics characteristics variations
668 within a tropical Alfisol in Southwestern Nigeria under different land use management, *Soil and Tillage*
669 *Research*, 182, 45–56, <https://doi.org/10.1016/j.still.2018.04.017>, 2018.

670 Greenwood: Land use and tillage effects on soil saturated hydraulic conductivity: Does infiltration
671 method matter?, Master Thesis, Lincoln University, New-Zeeland, 2017.

672 Fick, S. E. and Hijmans, R. J.: WorldClim 2: new 1-km spatial resolution climate surfaces for global land
673 areas, 37, 4302–4315, <https://doi.org/10.1002/joc.5086>, 2017.

674 Gupta, S., Hengl, T., Lehmann, P., Bonetti, S., and Or, D.: SoilKsatDB: global database of soil saturated
675 hydraulic conductivity measurements for geoscience applications, 13, 1593–1612,
676 <https://doi.org/10.5194/essd-13-1593-2021>, 2021a.

677 Gupta, S., Lehmann, P., Bonetti, S., Papritz, A., and Or, D.: Global Prediction of Soil Saturated
678 Hydraulic Conductivity Using Random Forest in a Covariate-Based GeoTransfer Function (CoGTF)
679 Framework, 13, e2020MS002242, <https://doi.org/10.1029/2020MS002242>, 2021b.

680 Hallam, J., Berdeni, D., Grayson, R., Guest, E. J., Holden, J., Lappage, M. G., Prendergast-Miller, M.
681 T., Robinson, D. A., Turner, A., Leake, J. R., and Hodson, M. E.: Effect of earthworms on soil physico-
682 hydraulic and chemical properties, herbage production, and wheat growth on arable land converted to
683 ley, *Science of The Total Environment*, 713, 136491, <https://doi.org/10.1016/j.scitotenv.2019.136491>,
684 2020.

685 Hardie, M. A., Doyle, R. B., Cotching, W. E., Mattern, K., and Lisson, S.: Influence of antecedent soil
686 moisture on hydraulic conductivity in a series of texture-contrast soils: INFLUENCE OF ANTECEDENT
687 SOIL MOISTURE ON HYDRAULIC CONDUCTIVITY, *Hydrol. Process.*, 26, 3079–3091,
688 <https://doi.org/10.1002/hyp.8325>, 2012.

689 Hillel, D.: *Introduction to Environmental Soil Physics*, Academic Press, Amsterdam, 2004.

690 Hirmas, D. R., Giménez, D., Nemes, A., Kerry, R., Brunzell, N. A., and Wilson, C. J.: Climate-induced
691 changes in continental-scale soil macroporosity may intensify water cycle, 561, 100–103,
692 <https://doi.org/10.1038/s41586-018-0463-x>, 2018.

693 Holden, J., Wearing, C., Palmer, S., Jackson, B., Johnston, K., and Brown, L. E.: Fire decreases near-
694 surface hydraulic conductivity and macropore flow in blanket peat: FIRE AND BLANKET PEAT
695 HYDROLOGY, *Hydrol. Process.*, 28, 2868–2876, <https://doi.org/10.1002/hyp.9875>, 2014.

696 Hyväluoma, J., Rätty, M., Kaseva, J., and Keskinen, R.: Changes over time in near-saturated hydraulic
697 conductivity of peat soil following reclamation for agriculture, 34, 237–243,
698 <https://doi.org/10.1002/hyp.13578>, 2020.

699 Iovino, M., Castellini, M., Bagarello, V., and Giordano, G.: Using Static and Dynamic Indicators to
700 Evaluate Soil Physical Quality in a Sicilian Area: SOIL PHYSICAL QUALITY EVALUATION BY STATIC

701 AND DYNAMIC INDICATORS, *Land Degrad. Develop.*, 27, 200–210, <https://doi.org/10.1002/ldr.2263>,
702 2016.

703 IUSS Working Group WRB: World Reference Base for Soil Resources 2014, Update 2015. International
704 Soil Classification System for Naming Soils and Creating Legends for Soil Maps., FAO, Rome, 2015.

705 Jarvis, N., Koestel, J., Messing, I., Moeys, J., and Lindahl, A.: Influence of soil, land use and climatic
706 factors on the hydraulic conductivity of soil, 17, 5185–5195, <https://doi.org/10.5194/hess-17-5185-2013>,
707 2013.

708 Jorda, H., Bechtold, M., Jarvis, N., and Koestel, J.: Using boosted regression trees to explore key
709 factors controlling saturated and near-saturated hydraulic conductivity, 66, 744–756,
710 <https://doi.org/10.1111/ejss.12249>, 2015.

711 Kelishadi, H., Mosaddeghi, M. R., Hajabbasi, M. A., and Ayoubi, S.: Near-saturated soil hydraulic
712 properties as influenced by land use management systems in Koohrang region of central Zagros, Iran,
713 *Geoderma*, 213, 426–434, <https://doi.org/10.1016/j.geoderma.2013.08.008>, 2014.

714 Keskinen, R., Rätty, M., Kaseva, J., and Hyväluoma, J.: Variations in near-saturated hydraulic
715 conductivity of arable mineral topsoils in south-western and central-eastern Finland, *AFSci*, 28,
716 <https://doi.org/10.23986/afsci.79329>, 2019.

717 Khetdan, C., Chittamart, N., Tawornpruek, S., Kongkaew, T., Onsamrarn, W., and Garré, S.: Influence
718 of rock fragments on hydraulic properties of Ultisols in Ratchaburi Province, Thailand, *Geoderma*
719 *Regional*, 10, 21–28, <https://doi.org/10.1016/j.geodrs.2017.04.001>, 2017.

720 Klute, A. and Dirksen, C.: Hydraulic conductivity and diffusivity: Laboratory measurements, in: *Methods*
721 *of soil analysis, Part 1, vol. 1*, edited by: Klute, A., Soil Science Society of America, Inc., Madison,
722 Wisconsin, USA, 687–734, 1986.

723 Koestel, J., Dathe, A., Skaggs, T. H., Klakegg, O., Ahmad, M. A., Babko, M., Giménez, D., Farkas, C.,
724 Nemes, A., and Jarvis, N.: Estimating the Permeability of Naturally Structured Soil From Percolation

725 Theory and Pore Space Characteristics Imaged by X-Ray, *Water Resources Research*, 54, 9255-9263,
726 2018.

727 Larsbo, M., Koestel, J., and Jarvis, N.: Relations between macropore network characteristics and the
728 degree of preferential solute transport, 18, 5255–5269, <https://doi.org/10.5194/hess-18-5255-2014>,
729 2014.

730 Larsbo, M., Sandin, M., Jarvis, N., Etana, A., and Kreuger, J.: Surface Runoff of Pesticides from a Clay
731 Loam Field in Sweden, *J. Environ. Qual.*, 45, 1367–1374, <https://doi.org/10.2134/jeq2015.10.0528>,
732 2016a.

733 Larsbo, M., Koestel, J., Kätterer, T., and Jarvis, N.: Preferential transport in macropores is reduced by
734 soil organic carbon, *Vadose Zone Journal*, 15, 2016b.

735 Lipiec, J. and Hatano, R.: Quantification of compaction effects on soil physical properties and crop
736 growth, *Geoderma*, 116, 107-136, 2003.

737 Logsdon, S. D. and Jaynes, D. B.: Methodology for Determining Hydraulic Conductivity with Tension
738 Infiltrimeters, 57, 1426–1431, <https://doi.org/10.2136/sssaj1993.03615995005700060005x>, 1993.

739 Lopes, V. S., Cardoso, I. M., Fernandes, O. R., Rocha, G. C., Simas, F. N. B., de Melo Moura, W.,
740 Santana, F. C., Veloso, G. V., and da Luz, J. M. R.: The establishment of a secondary forest in a
741 degraded pasture to improve hydraulic properties of the soil, *Soil and Tillage Research*, 198, 104538,
742 <https://doi.org/10.1016/j.still.2019.104538>, 2020.

743 Lozano, L. A., Germán Soracco, C., Buda, V. S., Sarli, G. O., and Filgueira, R. R.: Stabilization of soil
744 hydraulic properties under a long term no-till system, *Rev. Bras. Ciênc. Solo*, 38, 1281–1292,
745 <https://doi.org/10.1590/S0100-06832014000400024>, 2014.

746 Lozano-Baez, S. E., Cooper, M., Frosini de Barros Ferraz, S., Ribeiro Rodrigues, R., Castellini, M., and
747 Di Prima, S.: Assessing Water Infiltration and Soil Water Repellency in Brazilian Atlantic Forest Soils,
748 display, 2020.

749 Matula, S., Miháliková, M., Lufinková, J., and Bátková, K.: The role of the initial soil water content in the
750 determination of unsaturated soil hydraulic conductivity using a tension infiltrometer, *Plant Soil Environ.*,
751 61, 515–521, <https://doi.org/10.17221/527/2015-PSE>, 2015.

752 McBratney, A. B., Minasny, B., and Tranter, G.: Necessary meta-data for pedotransfer functions, 160,
753 627–629, <https://doi.org/10.1016/j.geoderma.2010.09.023>, 2011.

754 Meshgi, A. and Chui, T. F. M.: Analysing tension infiltrometer data from sloped surface using two-
755 dimensional approximation: ANALYSING TENSION INFILTROMETER DATA FROM SLOPED
756 SURFACE, *Hydrological Processes*, 28, 744–752, <https://doi.org/10.1002/hyp.9621>, 2014.

757 Messing, I. and Jarvis, N. J.: Seasonal variation in field-saturated hydraulic conductivity in two swelling
758 clay soils in Sweden, 41, 229–237, 1990.

759 Messing, I. and Jarvis, N.J.: Temporal variation in the hydraulic conductivity of a tilled clay soil as
760 measured by tension infiltrometers. *Journal of Soil Science*, 44, 11-24, 1993.

761 Meurer, K., Barron, J., Chenu, C., Coucheney, E., Fielding, M., Hallett, P., Herrmann, A. M., Keller, T.,
762 Koestel, J., Larsbo, M., Lewan, E., Or, D., Parsons, D., Parvin, N., Taylor, A., Vereecken, H., and Jarvis,
763 N.: A framework for modelling soil structure dynamics induced by biological activity, *Glob. Change Biol.*,
764 26, 5382–5403, <https://doi.org/10.1111/gcb.15289>, 2020.

765 Miller, J. J., Beasley, B. W., Drury, C. F., Larney, F. J., Hao, X., and Chanasyk, D. S.: Influence of long-
766 term feedlot manure amendments on soil hydraulic conductivity, water-stable aggregates, and soil
767 thermal properties during the growing season, *Can. J. Soil. Sci.*, 98, 421–435,
768 <https://doi.org/10.1139/cjss-2017-0061>, 2018.

769 Morris, P.J., Davies, M.L., Baird, A.J., Balliston, N., Bourgault, M.-A., Clymo, R.S., Fewster, R.E.,
770 Furukawa, A.K., Holden, J., Kessel, E., Ketcheson, S.J., Kløve, B., Larocque, M., Marttila, H., Menberu,
771 M.W., Moore, P.A., Price, J.S., Ronkanen, A.-K., Rosa, E., Strack, M., Surrridge, B.W.J., Waddington,
772 J.M., Whittington, P. and Wilkinson, S.L.: Saturated Hydraulic Conductivity in Northern Peats Inferred

773 From Other Measurements. *Water Resources Research*, **58**, <https://doi.org/10.1016/e2022WR033181>,
774 2022.

775 Nemes, A., Schaap, M. G., Leij, F. J., and Wosten, J. H. M.: Description of the unsaturated soil hydraulic
776 database UNSODA version 2.0, 251, 151–162, 2001.

777 Pagliai, M., Vignozzi, N., and Pellegrini, S.: Soil structure and the effect of management practices, *Soil
778 & Tillage Research*, 79, 131-143, 2004.

779 Poggio, L., de Sousa, L. M., Batjes, N. H., Heuvelink, G. B. M., Kempen, B., Ribeiro, E., and Rossiter,
780 D.: SoilGrids 2.0: producing soil information for the globe with quantified spatial uncertainty, *SOIL*, 7,
781 217-240, 2021.

782 Pulido Moncada, M., Helwig Penning, L., Timm, L. C., Gabriels, D., and Cornelis, W. M.: Visual
783 examinations and soil physical and hydraulic properties for assessing soil structural quality of soils with
784 contrasting textures and land uses, *Soil and Tillage Research*, 140, 20–28,
785 <https://doi.org/10.1016/j.still.2014.02.009>, 2014.

786 Rahbeh, M.: Characterization of preferential flow in soils near Zarqa river (Jordan) using in situ tension
787 infiltrometer measurements, 7, e8057, <https://doi.org/10.7717/peerj.8057>, 2019.

788 Rahmati, M., Weihermüller, L., Vanderborght, J., Pachepsky, Y. A., Mao, L., Sadeghi, S. H., Moosavi,
789 N., Kheirfam, H., Montzka, C., Van Looy, K., Toth, B., Hazbavi, Z., Al Yamani, W., Albalasmeh, A. A.,
790 Alghzawi, M. Z., Angulo-Jaramillo, R., Antonino, A. C. D., Arampatzis, G., Armindo, R. A., Asadi, H.,
791 Bamutaze, Y., Batlle-Aguilar, J., Béchet, B., Becker, F., Blöschl, G., Bohne, K., Braud, I., Castellano,
792 C., Cerdà, A., Chalhoub, M., Cichota, R., Císlarová, M., Clothier, B., Coquet, Y., Cornelis, W., Corradini,
793 C., Coutinho, A. P., De Oliveira, M. B., De Macedo, J. R., Durães, M. F., Emami, H., Eskandari, I.,
794 Farajnia, A., Flammini, A., Fodor, N., Gharaibeh, M., Ghavimipannah, M. H., Ghezzehei, T. A., Giertz,
795 S., Hatzigiannakis, E. G., Horn, R., Jiménez, J. J., Jacques, D., Keesstra, S. D., Kelishadi, H., Kiani-
796 Harchegani, M., Kouselou, M., Jha, M. K., Lassabatere, L., Li, X., Liebig, M. A., Lichner, L., López, M.
797 V., Machiwal, D., Mallants, D., Mallmann, M. S., De Oliveira Marques, J. D., Marshall, M. R., Mertens,

798 J., Meunier, F., Mohammadi, M. H., Mohanty, B. P., Pulido-Moncada, M., Montenegro, S., Morbidelli,
799 R., Moret-Fernández, D., Moosavi, A. A., Mosaddeghi, M. R., Mousavi, S. B., Mozaffari, H., Nabiollahi,
800 K., Neyshabouri, M. R., Ottoni, M. V., Ottoni Filho, T. B., Pahlavan-Rad, M. R., Panagopoulos, A., Peth,
801 S., Peyneau, P. E., Picciafuoco, T., Poesen, J., Pulido, M., Reinert, D. J., Reinsch, S., Rezaei, M.,
802 Roberts, F. P., Robinson, D., Rodrigo-Comino, J., Rotunno Filho, O. C., Saito, T., et al.: Development
803 and analysis of the Soil Water Infiltration Global database, 10, 1237–1263, [https://doi.org/10.5194/essd-](https://doi.org/10.5194/essd-10-1237-2018)
804 10-1237-2018, 2018.

805 Reynolds, W. D. and Elrick, D. E.: Determination of Hydraulic Conductivity Using a Tension Infiltrometer,
806 55, 633–639, <https://doi.org/10.2136/sssaj1991.03615995005500030001x>, 1991.

807 Rienzner, M. and Gandolfi, C.: Investigation of spatial and temporal variability of saturated soil hydraulic
808 conductivity at the field-scale, *Soil and Tillage Research*, 135, 28–40,
809 <https://doi.org/10.1016/j.still.2013.08.012>, 2014.

810 Sandin, M., Koestel, J., Jarvis, N., and Larsbo, M.: Post-tillage evolution of structural pore space and
811 saturated and near-saturated hydraulic conductivity in a clay loam soil, 165, 161–168,
812 <https://doi.org/10.1016/j.still.2016.08.004>, 1, 2017.

813 Schaap, M. G. and Leij, F. J.: Improved prediction of unsaturated hydraulic conductivity with the
814 Mualem-van Genuchten model, *Soil Science Society of America Journal*, 64 (3), pp. 843 – 851, 2000.

815 Schaap, M. G., Leij, F. J., and van Genuchten, M. T.: ROSETTA: a computer program for estimating
816 soil hydraulic parameters with hierarchical pedotransfer functions, *Journal of Hydrology*, 251, 163–176,
817 2001.

818 Schlüter, S., Albrecht, L., Schwärzel, K., and Kreiselmeier, J.: Long-term effects of conventional tillage
819 and no-tillage on saturated and near-saturated hydraulic conductivity – Can their prediction be improved
820 by pore metrics obtained with X-ray CT? *Geoderma*, 361, 2020.

821 Smettem, K. R. J. and Clothier, B. E.: Measuring unsaturated sorptivity and hydraulic conductivity using
822 multiple disc permeameters, 40, 563–568, <https://doi.org/10.1111/j.1365-2389.1989.tb01297.x>, 1989.

823 Soracco, C. G., Lozano, L. A., Villarreal, R., Palancar, T. C., Collazo, D. J., Sarli, G. O., and Filgueira,
824 R. R.: EFFECTS OF COMPACTION DUE TO MACHINERY TRAFFIC ON SOIL PORE
825 CONFIGURATION, *Rev. Bras. Ciênc. Solo*, 39, 408–415,
826 <https://doi.org/10.1590/01000683rbc20140359>, 2015.

827 Soracco, C. G., Villarreal, R., Melani, E. M., Oderiz, J. A., Salazar, M. P., Otero, M. F., Irizar, A. B., and
828 Lozano, L. A.: Hydraulic conductivity and pore connectivity. Effects of conventional and no-till systems
829 determined using a simple laboratory device, *Geoderma*, 337, 1236–1244,
830 <https://doi.org/10.1016/j.geoderma.2018.10.045>, 2019.

831 Tóth, B., Weynants, M., Nemes, A., Makó, A., Bilas, G., and Tóth, G.: New generation of hydraulic
832 pedotransfer functions for Europe, 66, 226–238, <https://doi.org/10.1111/ejss.12192>, 2015.

833 Trabucco, A. and Zomer, R.: Global Aridity Index and Potential Evapotranspiration (ET₀) Climate
834 Database, <https://doi.org/10.6084/m9.figshare.7504448.v3>, 2019.

835 Van Looy, K., Bouma, J., Herbst, M., Koestel, J., Minasny, B., Mishra, U., Montzka, C., Nemes, A.,
836 Pachepsky, Y. A., Padarian, J., Schaap, M. G., Toth, B., Verhoef, A., Vanderborght, J., van der Ploeg,
837 M. J., Weihermuller, L., Zacharias, S., Zhang, Y. G., and Vereecken, H.: Pedotransfer Functions in
838 *Earth System Science: Challenges and Perspectives*, 55, 1199–1256,
839 <https://doi.org/10.1002/2017rg000581>, 2017.

840 Vandervaere, J.-P., Vauclin, M., and Elrick, D. E.: Transient Flow from Tension Infiltrometers II. Four
841 Methods to Determine Sorptivity and Conductivity, 64, 1272–1284,
842 <https://doi.org/10.2136/sssaj2000.6441272x>, 2000.

843 Vereecken, H., Weynants, M., Javaux, M., Pachepsky, Y., Schaap, M. G., and Genuchten, M. T. v.:
844 Using pedotransfer functions to estimate the van Genuchten–Mualem soil hydraulic properties: A
845 review, *Vadose Zone Journal*, 9, 795–820, 2010.

846 Wang, L., Garré, S., De Cuyper, T., Pollet, S., Cornelis, W. unpublished data.

847 Wanniarachchi, D., Cheema, M., Thomas, R., Kavanagh, V., and Galagedara, L.: Impact of Soil
848 Amendments on the Hydraulic Conductivity of Boreal Agricultural Podzols, *Agriculture*, 9, 133,
849 <https://doi.org/10.3390/agriculture9060133>, 2019.

850 Weynants, M., Vereecken, H., and Javaux, M.: Revisiting Vereecken pedotransfer functions:
851 Introducing a closed-form hydraulic model, 8, 86–95, <https://doi.org/10.2136/vzj2008.0062>, 2009.

852 Weynants, M., Montanarella, L., Toth, G., Arnoldussen, A., Anaya Romero, M., Bilas, G., Borresen, T.,
853 Cornelis, W., Daroussin, J., Feichtinger, F., Gonçalves, M., Hannam, J., Haugen, L., Hennings, V.,
854 Houskova, B., Iovino, M., Javaux, M., Keay, C., Kätterer, T., Kvaerno, S., Laktinova, T., Lamorski, K.,
855 Lilly, A., Mako, A., Matula, S., Morari, F., Nemes, A., Nyborg, Å., Patyka, N., Riley, H., Romano, N.,
856 Schindler, U., Shein, E., Slawinski, C., Strauss, P., Tóth, B., and Woesten, H.: European
857 HYdropedological Data Inventory (EU-HYDI). EUR 26053, Publications Office of the European Union,
858 Luxembourg (Luxembourg). JRC81129., 2013.

859 Whalley, W. R., Dumitru, E., and Dexter, A. R.: Biological effects of soil compaction, *Soil and Tillage*
860 *Research*, 35, 53-68, 1995.

861 Wösten, J. H. M., Lilly, A., Nemes, A., and le Bas, C.: Development and use of a database of hydraulic
862 properties of European soils, 90, 169–185, 1999.

863 Wösten, J. H. M., Pachepsky, Y. A., and Rawls, W. J.: Pedotransfer functions: bridging the gap between
864 available basic soil data and missing soil hydraulic characteristics, 251, 123–150,
865 [https://doi.org/10.1016/S0022-1694\(01\)00464-4](https://doi.org/10.1016/S0022-1694(01)00464-4), 2001.

866 Wooding, R. A.: Steady Infiltration from a Shallow Circular Pond, *Water Resources Research*, 4, 1259-
867 1273, 1968.

868 Yu, Z., Dong, W., Young, M. H., Li, Y., and Yang, T.: On evaluating characteristics of the solute transport
869 in the arid vadose zone, 52, 50–62, <https://doi.org/10.1111/gwat.12026>, 2014.

870 Yusuf, K. O., Ejeji, C. J., and Baiyeri, M. R.: Determination of sorptivity, infiltration rate and hydraulic
871 conductivity of soil using a tension infiltrometer, 10, 99–108, 2018.

872 Yusuf, K. O., Obalowu, R. O., Akinleye, G. T., and Adio-Yusuf, S. I.: Determination of Sorptivity,
873 Infiltration Rate and Hydraulic Conductivity of Loamy Sand using Tension Infiltration and Double-Ring
874 Infiltration, FUOYEJET, 5, <https://doi.org/10.46792/fuoyejet.v5i2.501>, 2020.

875 Zeng, C., Zhang, F., Wang, Q., Chen, Y., and Joswiak, D. R.: Impact of alpine meadow degradation on
876 soil hydraulic properties over the Qinghai-Tibetan Plateau, Journal of Hydrology, 478, 148–156,
877 <https://doi.org/10.1016/j.jhydrol.2012.11.058>, 2013a.

878 Zeng, C., Wang, Q., Zhang, F., and Zhang, J.: Temporal changes in soil hydraulic conductivity with
879 different soil types and irrigation methods, Geoderma, 193–194, 290–299,
880 <https://doi.org/10.1016/j.geoderma.2012.10.013>, 2013b.

881 Zhang, R.: Determination of Soil Sorptivity and Hydraulic Conductivity from the Disk Infiltration, 61,
882 1024–1030, <https://doi.org/10.2136/sssaj1997.03615995006100040005x>, 1997.

883 Zhang, Y., Zhao, W., Li, X., Jia, A., and Kang, W.: Contribution of soil macropores to water infiltration
884 across different land use types in a desert–oasis ecoregion, Land Degrad Dev, 32, 1751–1760,
885 <https://doi.org/10.1002/ldr.3823>, 2021.

886 Zhang, Z., Lin, L., Wang, Y., and Peng, X.: Temporal change in soil macropores measured using tension
887 infiltrometer under different land uses and slope positions in subtropical China, J Soils Sediments, 16,
888 854–863, <https://doi.org/10.1007/s11368-015-1295-z>, 2016.

889 Zhang, Z. B., Zhou, H., Zhao, Q. G., Lin, H., and Peng, X.: Characteristics of cracks in two paddy soils
890 and their impacts on preferential flow, Geoderma, 228–229, 114–121,
891 <https://doi.org/10.1016/j.geoderma.2013.07.026>, 2014.

- 892 Zhang, Z.-H., Li, X.-Y., Jiang, Z.-Y., Peng, H.-Y., Li, L., and Zhao, G.-Q.: Changes in some soil
893 properties induced by re-conversion of cropland into grassland in the semiarid steppe zone of Inner
894 Mongolia, China, *Plant Soil*, 373, 89–106, <https://doi.org/10.1007/s11104-013-1772-3>, 2013.
- 895 Zhao, X., Wu, P., Gao, X., Tian, L., and Li, H.: Changes of soil hydraulic properties under early-stage
896 natural vegetation recovering on the Loess Plateau of China, *CATENA*, 113, 386–391,
897 <https://doi.org/10.1016/j.catena.2013.08.023>, 2014.
- 898 Zhou, B. B., Wang, Q. J., and Wu, X. B.: Optimal disc tension infiltrometer estimation techniques for
899 hydraulic properties of soil under different land uses, 9, 92–98,
900 <https://doi.org/10.3965/j.ijabe.20160904.2161>, 2016.
- 901 کریمی‌ان, ن.: اثر روش‌های خاک‌ورزی و مدیریت بقایای گیاهی and , میرزاوند, ج., موسوی, س. ع., ا., ثامنی, ع., افضل‌ی‌نیا, ص
902 , برهدایت هیدرولیکی غیر اشباع خاک در تناوب گندم – ذرت, مجله پژوهش‌های حفاظت آب و خاک, 23
903 <https://doi.org/10.22069/jwfst.2016.3190>, 2016.